

## Cinnamic Anilides as New Mitochondrial Permeability Transition Pore Inhibitors Endowed with Ischemia-Reperfusion Injury Protective Effect in Vivo

Daniele Fancelli,<sup>\*,†,○</sup> Agnese Abate,<sup>‡,◆</sup> Raffaella Amici,<sup>†,○</sup> Paolo Bernardi,<sup>⊥</sup> Marco Ballarini,<sup>†,§</sup> Anna Cappa,<sup>‡,○</sup> Giacomo Carenzi,<sup>‡,¶</sup> Andrea Colombo,<sup>∇,+</sup> Cristina Contursi,<sup>†,▲</sup> Fabio Di Lisa,<sup>#</sup> Giulio Dondio,<sup>∇,□</sup> Stefania Gagliardi,<sup>∇,◇</sup> Eva Milanese,<sup>†</sup> Saverio Minucci,<sup>§,||</sup> Gilles Pain,<sup>†,△</sup> Pier Giuseppe Pelicci,<sup>§</sup> Alessandra Saccani,<sup>†,■</sup> Mariangela Storto,<sup>†,§</sup> Florian Thaler,<sup>†,○</sup> Mario Varasi,<sup>‡,○</sup> Manuela Villa,<sup>†,○</sup> and Simon Plyte<sup>†,●</sup>

<sup>†</sup>Genextra Group, Congenia s.r.l., Via Adamello 16, 20139 Milan, Italy

<sup>‡</sup>Genextra Group, DAC s.r.l., Via Adamello 16, 20139 Milan, Italy

<sup>§</sup>Department of Experimental Oncology, European Institute of Oncology IEO, Via Adamello 16, 20139 Milan, Italy

<sup>||</sup>Department of Biosciences, University of Milan, 20100 Milan, Italy

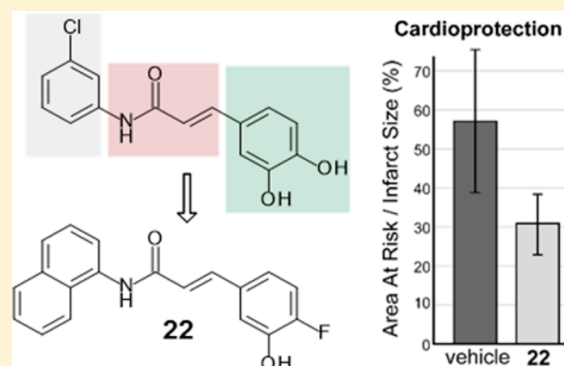
<sup>⊥</sup>Department of Biomedical Sciences, University of Padua, Via Ugo Bassi 58/B, 35121 Padua, Italy

<sup>#</sup>Department of Biomedical Sciences, University of Padua, Viale G. Colombo 3, 35131 Padua, Italy

<sup>∇</sup>NiKem Research s.r.l., Via Zambelletti 25, 20021 Baranzate, MI, Italy

**S** Supporting Information

**ABSTRACT:** In this account, we report the development of a series of substituted cinnamic anilides that represents a novel class of mitochondrial permeability transition pore (mPTP) inhibitors. Initial class expansion led to the establishment of the basic structural requirements for activity and to the identification of derivatives with inhibitory potency higher than that of the standard inhibitor cyclosporine-A (CsA). These compounds can inhibit mPTP opening in response to several stimuli including calcium overload, oxidative stress, and thiol cross-linkers. The activity of the cinnamic anilide mPTP inhibitors turned out to be additive with that of CsA, suggesting for these inhibitors a molecular target different from cyclophillin-D. In vitro and in vivo data are presented for (*E*)-3-(4-fluoro-3-hydroxyphenyl)-*N*-naphthalen-1-yl-acrylamide **22**, one of the most interesting compounds in this series, able to attenuate opening of the mPTP and limit reperfusion injury in a rabbit model of acute myocardial infarction.



## INTRODUCTION

The mitochondrial permeability transition (mPT) is a phenomenon whereby the inner mitochondrial membrane becomes permeable to solutes. This induces cessation of mitochondrial respiration and energy production, mitochondrial swelling and outer membrane rupture, release of apoptotic factors, and cell death leading to organ damage. The mPT is mediated by opening of a nonselective pore within the mitochondria: the mitochondrial permeability transition pore (mPTP). Even after intensive investigation, the exact molecular nature of the mPTP is still not known.<sup>1</sup> Several proteins have been implicated in facilitating the mPTP: adenine nucleotide transporter, phosphate carrier protein, cyclophilin D, and recently the F<sub>1</sub>F<sub>0</sub> ATP synthase complex, but no single protein has been unambiguously demonstrated to be the pore-forming unit.<sup>2–5</sup> However, strong evidence now points to pore

formation by dimers of the ATP synthase.<sup>4</sup> Much of our understanding of the functioning of the mPTP comes from studies using the immunosuppressive agent 47 (cyclosporine A, CsA)<sup>6</sup> (Figure 1), which in the late 1980s was discovered to inhibit the mPTP, as well as from cyclophilin D knockout mice.<sup>7</sup> Opening of the mPTP can be induced by calcium (Ca<sup>2+</sup>) overload and reactive oxygen species (ROS). These conditions are common to several diseases including reperfusion injury (angioplasty after a heart attack, transplantation surgery, and stroke), neurological diseases such as amyloid lateral sclerosis and Alzheimer's disease, traumatic brain injury, dystrophies, and myopathies.<sup>8–11</sup> In essence, prolonged opening of the mPTP can have catastrophic effects on organ function in many

Received: March 13, 2014

Published: June 11, 2014

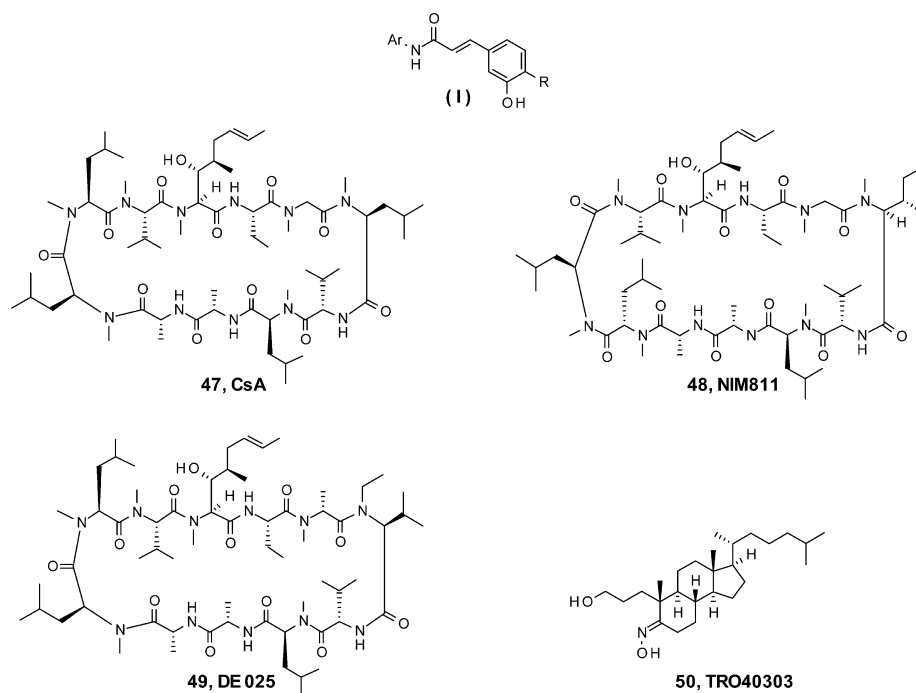


**Figure 1.** Chemical structures of cinnamic anilides (I) and known mPTP inhibitors.

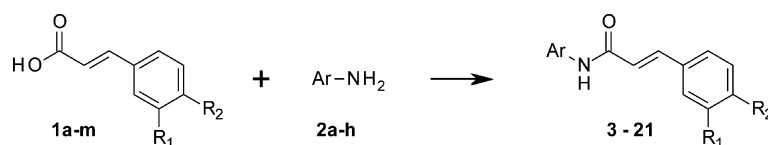
diverse diseases. In particular, opening of the mPTP is considered to be a key to the immediate tissue damage caused by reperfusion of ischemic tissue.<sup>12</sup> In the case of acute myocardial infarction (AMI), the reperfusion of ischemic tissue causes cardiomyocyte damage and contributes to final infarct size. Studies in animal models suggest that lethal reperfusion injury (LRI) may contribute up to 50% of the final infarct size.<sup>12,13</sup> Indeed, this form of myocardial injury may in part explain why, even after optimal myocardial reperfusion, the death rate is still approximately 10% and the incidence of cardiac failure remains almost 20%.<sup>14</sup> Currently, there are no registered therapies for the treatment of LRI.<sup>15,16</sup> Hence, inhibition of opening of the mPTP upon tissue reperfusion should attenuate lethal reperfusion injury and reduce final infarct size, thus permitting the full realization of the benefits of reperfusion strategies in AMI. Consistent with this hypothesis, Piot et al. demonstrated in a proof-of-concept study that administration of CsA to patients with ST-elevated myocardial infarction 5 min prior to PCI significantly reduced troponin I and creatinine kinase release, indicative of reduced cardiac damage.<sup>17</sup> Larger clinical studies are currently underway to confirm this initial observation. Despite its usefulness as an investigational tool, the use of CsA in therapy could be severely limited by several factors, such as its multiple pharmacological activities, well documented adverse effects,<sup>18,19</sup> and risk of cardiovascular side effects induced by the cremophor formulation.<sup>20,21</sup>

Nonimmunosuppressive cyclosporin A analogues such as the antiviral agents **48** (NIM811) and **49** (Debio 025) (Figure 1) retain cyclophilin D inhibitory activity and consequently inhibit mPTP, but their potency is restricted by the limits of the regulatory role of cyclophilin D in mPTP function and its level of expression.<sup>22,23</sup> Compound **49** was demonstrated to protect mouse dystrophic cells against mitochondria-mediated death and showed efficacy in mouse models of collagen VI<sup>24</sup> and Duchenne muscular dystrophy,<sup>25</sup> suggesting that therapies targeting the mPTP may be helpful to patients. In addition, **49**

administered to mice undergoing myocardial infarction rescued cardiac function compared to sham operated mice.<sup>23</sup> The cholesterol-oxime **50** (TRO40303) (Figure 1) specifically binds to the cholesterol site of the mitochondrial translocator protein (18 kDa)<sup>26</sup> (TSPO), which is potentially involved in mPTP regulation.<sup>27</sup> Compound **50** demonstrated cardioprotective properties in preclinical models<sup>26</sup> and is currently being evaluated for reduction of reperfusion injury in acute ST-elevation myocardial infarction patients in a phase II proof-of-concept clinical study.<sup>28</sup>

Because of the extremely high therapeutic potential of mPTP inhibition and the paucity and limitations of known inhibitors, we embarked on a program aimed at identifying and developing novel, selective, nonpeptide inhibitors of the mPTP. In this article, we describe the synthesis, the structure–activity relationships (SAR) for inhibition of mPTP opening induced by calcium overload, and a preliminary biological characterization of cinnamic anilides (I), a novel series of potent inhibitors of mPTP.

The parent compound of this series (**3**), the 3-chlorophenyl anilide of caffeic acid, was originated by a high-throughput screen (data not shown) carried out to identify compounds able to inhibit the swelling induced by calcium overload in mitochondrial preparations from rat liver. Subsequent class expansion led to the establishment of the basic structural requirements for activity and to the identification of derivatives with inhibitory potency higher than that of the standard inhibitor CsA. These compounds can inhibit mPTP opening in response to several stimuli including calcium overload, oxidative stress, and cross-linkers. Further, *in vitro* and *in vivo* data are presented for the representative compound (*E*)-3-(4-fluoro-3-hydroxy-phenyl)-*N*-naphthalen-1-yl-acrylamide (**22**) that show the potential of these inhibitors to attenuate opening of the mPTP and their ability to limit reperfusion injury in a rabbit model of acute myocardial infarction.

Scheme 1<sup>a</sup>

	R <sub>1</sub>	R <sub>2</sub>		Ar	coupling <sup>a</sup>	product
<b>1a</b>	OH	OH	<b>2a</b>	3-Cl-Ph	A	<b>3</b>
<b>1b</b>	OH	H	<b>2a</b>	3-Cl-Ph	B	<b>4</b>
<b>1c</b>	H	OH	<b>2a</b>	3-Cl-Ph	A	<b>5</b>
<b>1d</b>	OH	OMe	<b>2a</b>	3-Cl-Ph	B	<b>6</b>
<b>1e</b>	OMe	OH	<b>2a</b>	3-Cl-Ph	A	<b>7</b>
<b>1f</b>	OMe	OMe	<b>2a</b>	3-Cl-Ph	B	<b>8</b>
<b>1g</b>	F	H	<b>2a</b>	3-Cl-Ph	B	<b>9</b>
<b>1h</b>	NO <sub>2</sub>	H	<b>2a</b>	3-Cl-Ph	E	<b>10a</b>
<b>1i</b>	NHSO <sub>2</sub> Me	H	<b>2a</b>	3-Cl-Ph	C	<b>11</b>
<b>1j</b>	-NH-CH=CH-		<b>2a</b>	3-Cl-Ph	D	<b>12</b>
<b>1k</b>	OH	Me	<b>2a</b>	3-Cl-Ph	B	<b>13</b>
<b>1l</b>	OH	NO <sub>2</sub>	<b>2a</b>	3-Cl-Ph	B	<b>14a</b>
<b>1e</b>	OH	OMe	<b>2b</b>	3-Br-Ph	B	<b>15</b>
<b>1d</b>	OH	OMe	<b>2c</b>	3-OMe-Ph	B	<b>16</b>
<b>1d</b>	OH	OMe	<b>2d</b>	3-OiPr-Ph	B	<b>17</b>
<b>1d</b>	OH	OMe	<b>2e</b>	3-NO <sub>2</sub> -Ph	B	<b>18a</b>
<b>1d</b>	OH	OMe	<b>2f</b>	3-NMe <sub>2</sub> -Ph	B	<b>19</b>
<b>1d</b>	OH	OMe	<b>2g</b>	2-Cl-Ph	B	<b>20</b>
<b>1d</b>	OH	OMe	<b>2h</b>	4-Cl-Ph	B	<b>21</b>
<b>1m</b>	OH	F	<b>2i</b>	1-naphthyl	B	<b>22</b>
<b>1m</b>	OH	F	<b>2a</b>	3-Cl-Ph	B	<b>23</b>

<sup>a</sup>Reagents and conditions: coupling method A, ArNH<sub>2</sub>, DCC, THF, reflux; coupling method B, (i) SOCl<sub>2</sub>, THF, 50 °C, (ii) ArNH<sub>2</sub>, NEt<sub>3</sub>, THF, 0 °C to rt; coupling method C, (i) (COCl)<sub>2</sub>, DCM, reflux, (ii) ArNH<sub>2</sub>, NEt<sub>3</sub>, DCM, 0 °C to rt; coupling method D, ArNH<sub>2</sub>, EDC, HOBT, DCM, 0 °C to rt; coupling method E, (i) SOCl<sub>2</sub>, reflux, (ii) ArNH<sub>2</sub>, pyridine, 85 °C.

## CHEMISTRY

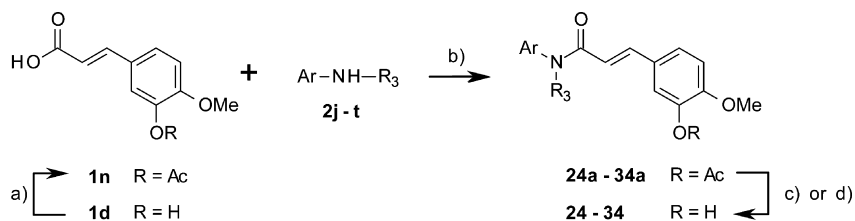
Most of the cinnamic amides **3–34** were directly obtained by standard coupling reactions (Scheme 1) carried out on the commercially available carboxylic acids **1a–m** and anilines **2a–t**. Specifically, the carboxylic acids were either activated with SOCl<sub>2</sub> (method B) or (COCl)<sub>2</sub> (method C) to form their acyl chlorides and then coupled with the anilines or the acids were directly reacted with the anilines in the presence of DCC (method A) or EDC/HOBT (method D). In some cases, the phenolic moiety of the 3-hydroxy-4-methoxy-cinnamic acid **1d** was first protected as an acetate (Scheme 2).

Compounds **10**, **14**, and **18** were obtained by reduction of the corresponding nitro derivatives **10a**, **14a**, and **18a**, respectively (Scheme 3). Attempts to prepare compound **37**

by direct coupling of the Weinreb amide of 2-(3-hydroxy-4-methoxyphenyl)cyclopropanecarboxylic acid (**36**) were unsuccessful, thus the amide was hydrolyzed to the corresponding carboxylic acid, activated with EDC and HOBT, and finally coupled with 3-chloroaniline **2a** (Scheme 4).

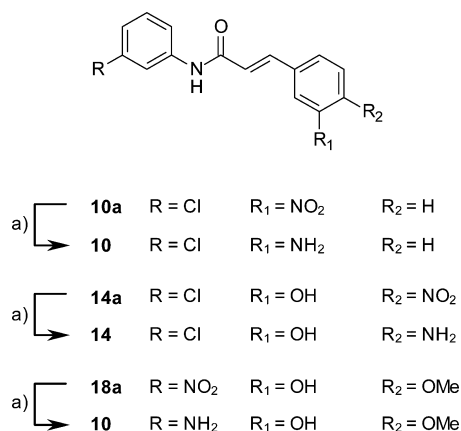
*N*-3-Acetoxy-4-methoxyphenyl-*N'*-3-Cl-benzoylthiourea **40**, obtained by the reaction of the 3-Cl-aniline **2a** and 3-acetyl-4-methoxy benzoyl isothiocyanate **39**, was converted into the amino-triazole derivative **41** by condensation with hydrazine and a concomitant loss of the acetyl protecting group (Scheme 5).

The 1,3,4-oxadiazole analogue **44** was prepared in two steps by coupling 3-chlorobenzoic acid hydrazide **42** and 3-acetyl-4-methoxy-cinnamic acid **1n** followed by alkaline hydrolysis of

Scheme 2<sup>a</sup>

	Ar	R <sub>3</sub>	product <sup>a</sup>
2j	3-CONH <sub>2</sub> -Ph	H	24
2k	3,4-Cl-Ph	H	25
2l	3-Cl-4-OMe-Ph	H	26
2m	3-Cl-2-OMe-Ph	H	27
2n		H	28
2o		H	29
2p		H	30
2q		H	31
2r		H	32
2s		H	33
2t	3-Cl-Ph	Me	34

<sup>a</sup>Reagents and conditions: (a) (i) NaH, THF, 0 °C, (ii) Ac<sub>2</sub>O reflux; (b) (i) SOCl<sub>2</sub>, THF, reflux, (ii) ArNHR<sub>3</sub>, DIPEA, THF, reflux; (c) HCl, MeOH, THF, rt; (d) (i) NaOH<sub>aq</sub> MeOH, reflux, (ii) HCl<sub>aq</sub>.

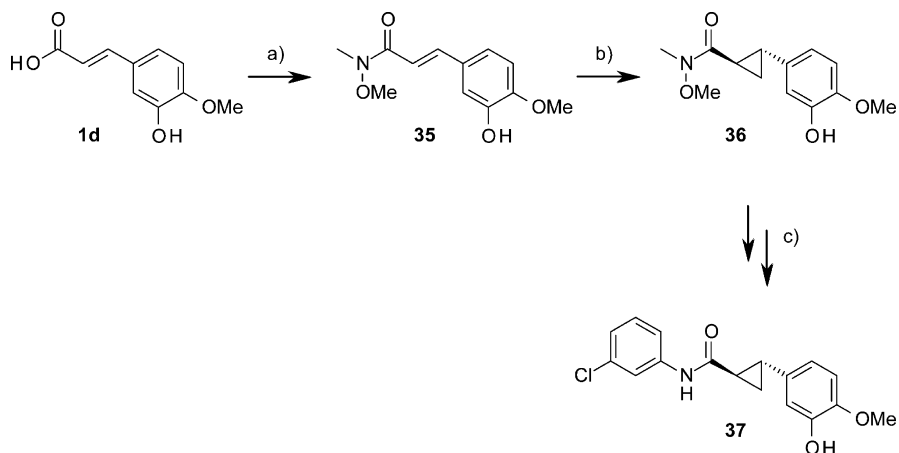
Scheme 3<sup>a</sup>

<sup>a</sup>Reagents and conditions: (a) SnCl<sub>2</sub>·2H<sub>2</sub>O, EtOH, EtOAc, reflux, 1.5–7 h.

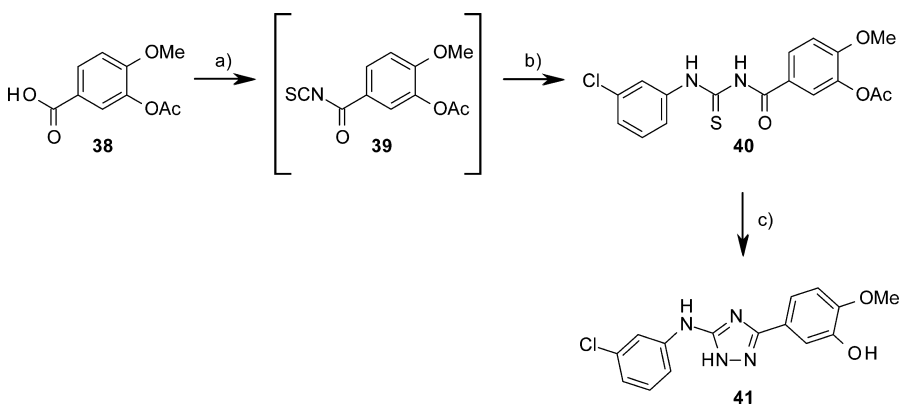
the acetate protecting group (Scheme 6). Finally, the phenylpropanoic analogue **46** was obtained by coupling the corresponding 3-hydroxy-4-methoxy-phenylpropanoic acid **45** that was activated with SOCl<sub>2</sub> and then treated with 3-chloroaniline **2a**.

### ■ SAR

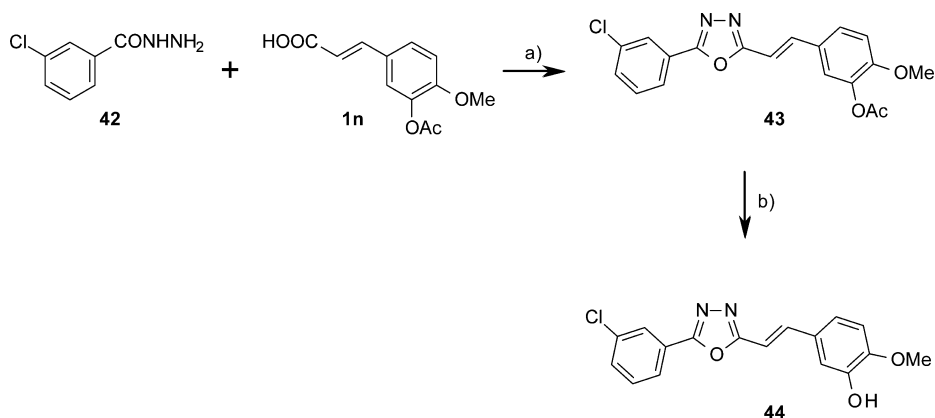
The mPTP inhibitory activity of cinnamic anilides **3–34** was initially evaluated by measuring their ability to protect murine mitochondria from mPTP opening induced by the exposure to increasing concentrations of Ca<sup>2+</sup> (calcium retention capacity assay (CRC)). This method allows measuring of the propensity of mitochondria to open the mPTP after calcium uptake. In the presence of extra-mitochondrial calcium, isolated mitochondria take up calcium into the matrix via the calcium uniporter. Continued addition of extra-mitochondrial calcium and subsequent uptake leads to the calcium-induced opening of the mPTP, mitochondrial depolarization, and release of stored calcium. The total amount of calcium that can be retained until calcium-induced mPTP opening occurs is termed the calcium retention capacity.<sup>29</sup> An example of the calcium retention

Scheme 4. Synthesis of Racemic *trans*-Cyclopropane Analogue<sup>a</sup>

<sup>a</sup>Reagents and conditions: (a) Me-NH-OMe-HCl, EDC, HOBT, DCM, rt, 16 h; (b) (i) NaH, Me<sub>3</sub>SO<sup>+</sup>I<sup>-</sup>, DMSO, rt, 16 h, (ii) HCl<sub>aq</sub>; (c) (i) tBuOK, H<sub>2</sub>O, Et<sub>2</sub>O, rt, 20 h, (ii) 3-ClPhNH<sub>2</sub>, EDC, HOBT, DCM, rt, 36 h.

Scheme 5<sup>a</sup>

<sup>a</sup>Reagents and conditions: (a) (i) SOCl<sub>2</sub>, DMF, THF, reflux, 2 h, (ii) KSCN, MeCN, reflux, 2 h; (b) 3-Cl-aniline, MeCN, 0.5 h, rt; (c) NH<sub>2</sub>NH<sub>2</sub>, CHCl<sub>3</sub>, reflux, 2 h.

Scheme 6<sup>a</sup>

<sup>a</sup>Reagents and conditions: (a) POCl<sub>3</sub>, 1,4-dioxane, reflux, 1 h; (b) 4N HCl, 1,4-dioxane, MeOH, rt.

capacity assay using the well-characterized mPTP inhibitor CsA is shown in Figure 2.

Measuring the increase of calcium needed to induce the mPTP in mitochondria treated with mPTP inhibitor vs untreated mitochondria (Ca<sup>2+</sup> overloading, μM) is a convenient and sensitive assay for assessing the ability of the compounds to

inhibit mPTP opening. The ratio between the amount of calcium required to trigger mPT in the presence of the compound (CRC<sub>i</sub>) with respect to that required to induce mPT in the absence of the compound (CRC<sub>o</sub>) is a measure of the inhibitory effect of the compound on the mPTP.

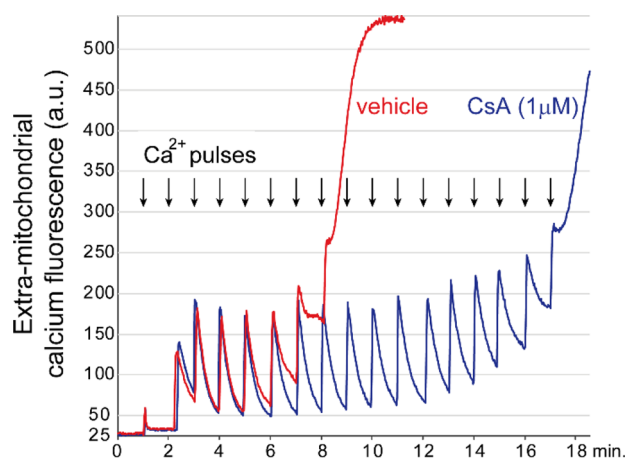


**Figure 2.** Calcium retention capacity assay.  $\text{CaCl}_2$  ( $1 \mu\text{L}$  of  $2 \text{ mM}$  stock solution) was added every minute to mouse liver mitochondria ( $200 \mu\text{L}$  of a  $0.5 \text{ mg/mL}$  suspension) in the presence of the fluorescent  $\text{Ca}^{2+}$  indicator Calcium Green 5N. Calcium uptake was followed by measuring extra-mitochondrial calcium green fluorescence until mPTP opening was achieved. CsA ( $1 \mu\text{M}$ ) was added to the mitochondria immediately prior to the start of the experiment.

All the cinnamic anilides here described were tested in the CRC assay in a dose escalation series at  $0.1$ ,  $0.5$ ,  $1$ , and  $5 \mu\text{M}$ . Because no significant differences were observed in the potency ranking of the compounds tested at different concentrations (see Supporting Information for the complete result data set), only the CRC values measured at  $1 \mu\text{M}$  inhibitor concentration are reported in the following SAR tables.

In the absence of structural information on the binding mode of these cinnamic anilides to their target mPTP component, we first performed a limited SAR investigation to identify the structural elements of the hit compound **3** that are essential for mPTP inhibition.

The structure of **3** was divided into three regions, namely the cinnamic phenyl ring, the central linker, and the aniline aryl ring (Figure 3), and systematic variations were carried out in each region.

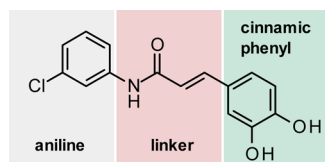


**Figure 3.** Regions of the structure of the hit compound **3** subjected to separate SAR investigation.

For this purpose and as the first attempt, the influence of the vicinal hydroxy moieties at the cinnamic phenyl ring was investigated (Table 1). The comparison of the activities of compounds **4** vs **5** and **6** vs **7** immediately suggests a crucial role for the hydroxyl group at position 3. This was further confirmed by the complete inactivity of compounds **9–12**, wherein the 3-hydroxyl is replaced by potential bioisosters such as fluorine, amino, or sulfonamido groups. In contrast, replacement of the hydroxyl at position 4 with different moieties (compounds **4**, **6**, **13**, **14**, and **23**) was better tolerated and the modifications variously modulated the potency. The most active example in this series resulted to be the 3-OH-4-OMe derivative **6**, which demonstrated potency comparable to

**Table 1.** *N*-(3-Chlorophenyl)cinnamic Anilides

compd	R <sub>1</sub>	R <sub>2</sub>	CRC <sub>i</sub> /CRC <sub>0</sub> (%) <sup>a</sup>	SD <sup>b</sup>
CsA			224	12
<b>3</b>	OH	OH	155	12
<b>4</b>	OH	H	136	12
<b>5</b>	H	OH	87	8.9
<b>6</b>	OH	OMe	186	14
<b>7</b>	OMe	OH	93	11
<b>8</b>	OMe	OMe	75	6.2
<b>9</b>	F	H	90	10
<b>10</b>	NH <sub>2</sub>	H	94	8.6
<b>11</b>	SO <sub>2</sub> NHMe	H	91	8.1
<b>12</b>	–NHCH=CH–		87	8.4
<b>13</b>	OH	Me	133	11
<b>14</b>	OH	NH <sub>2</sub>	102	10
<b>23</b>	OH	F	175	16

<sup>a</sup>Increase of the calcium retention capacity of mouse liver mitochondria after incubation with  $1 \mu\text{M}$  inhibitor. <sup>b</sup> $n = 3$ .

that of the reference standard CsA and was used for the very initial characterization of the mPTP inhibitory properties of the class. Thus, we decided to fix the right-hand side of compound **6** with the 3-OH-4-OMe moiety while exploring different central linkers and anilines.

The impact of the central linker on the activity of the compounds was explored starting from analogue **6**, but all the modifications introduced in this region such as *N*-methylation (**34**), double bond reduction (**46**), cyclopropanation (**37**), or cyclization (**41**, **44**) completely abolished activity (Table 2).

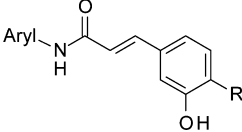
Finally, the effect of different anilines was investigated (Table 3, **15–33**). For this purpose, the 3-hydroxy-4-methoxy-cinnamic moiety was kept fixed. Far from being exhaustive, this initial exploration suggests that, while the chlorine present in the initial hit turned out to be the best among the residues

**Table 2.** Modification of the Central Linker

compd	structure	CRC <sub>i</sub> /CRC <sub>0</sub> % <sup>a</sup>	SD <sup>b</sup>
<b>6</b>		186	14
<b>34</b>		103	8.9
<b>37</b>		106	10
<b>41</b>		107	11
<b>44</b>		106	11
<b>46</b>		108	11

<sup>a</sup>Increase of the calcium retention capacity of mouse liver mitochondria after incubation with  $1 \mu\text{M}$  inhibitor. <sup>b</sup> $n = 3$ .

Table 3. 3-Hydroxycinnamic Anilides



compd	Aryl	R	CRC <sub>i</sub> /CRC <sub>0</sub> % <sup>a</sup>	SD <sup>b</sup>
6	3-Cl-Ph	OMe	186	14
15	3-Br-Ph	OMe	139	11
16	3-OMe-Ph	OMe	170	14
17	3-O <i>i</i> Pr-Ph	OMe	116	10
18	3-NH <sub>2</sub> -Ph	OMe	106	9.0
19	3-NMe <sub>2</sub> -Ph	OMe	114	8.8
24	3-CONH <sub>2</sub> -Ph	OMe	115	13
20	2-Cl-Ph	OMe	165	19
21	4-Cl-Ph	OMe	194	17
25	3,4-Cl-Ph	OMe	216	22
26	3Cl-4OMePh	OMe	196	15
27	3Cl-2OMePh	OMe	158	14
28		OMe	219	17
29		OMe	201	16
30		OMe	358	28
31		OMe	147	12
32		OMe	115	8.8
33		OMe	176	20
22		F	413	33

<sup>a</sup>Increase of the calcium retention capacity of mouse liver mitochondria after incubation with 1  $\mu$ M inhibitor. <sup>b</sup>*n* = 3.

explored at position 3 of the phenyl ring (6, 15–19, 24), this region of the scaffold tolerates a wide range of modifications. In fact, phenyl substitution at positions 2 and 4 (20, 21), phenyl disubstitution (25–27), and replacement of the phenyl with bicyclic moieties (28–33) led to compounds with maintained or improved potency.

In summary, the above findings allowed us to identify the phenol at position 3 of the cinnamic phenyl ring and the acrylamido linker as the structural determinants for the activity of this novel class of mPTP inhibitors, while modifications in the aniline region of the scaffold as well as position 4 of the cinnamic phenyl showed to be well tolerated and thus usable for the optimization of potency and properties.

Searching for a lead compound more potent than the initial lead 6, we drew our attention to the high potency showed by the naphthyl derivative 30 and investigated the effect of the introduction of heteroatoms in the bicyclic ring (31–33) as

well as the replacement of the methoxy moiety with fluorine (22). In the latter case, the aim was to reduce lipophilicity and potential metabolic liabilities of the molecule. While the heterobicyclic derivatives were less active, the fluorine analogue 22 showed the highest potency in the series and was selected as a class representative compound for a deeper biological characterization.

## BIOLOGY

Typically, opening of the mPTP in isolated mitochondria can be achieved by challenging the mitochondria with high Ca<sup>2+</sup> concentrations and can be assayed spectrophotometrically by monitoring the decrease of absorbance at 540 nm (A540), which indicates mitochondrial swelling as a result of solute influx into the mitochondrial matrix via the open mPTP.

In addition, the mPTP opening can be induced by challenging isolated mitochondria with oxidizing agents (e.g., diamide or menadione) or uncouplers of electron transport (e.g., trifluorocarbonylcyanide phenylhydrazone (FCCP)). In a preliminary assessment of the mechanism of action of this novel class of inhibitors, compound 6 was tested in this swelling assay for its ability to prevent mPTP opening in response to the different stimuli mentioned above in isolated mouse liver mitochondria. The results reported in Figure 4 show that cinnamic anilides prevent mPTP opening induced by stimuli independent of changes in calcium flux, thus suggesting that they behave as genuine inhibitors of the mPTP and not of calcium homeostasis (Figure 4B–D).

Because the cinnamide skeleton is present in diverse compounds with a wide range of pharmacological activities,<sup>30–34</sup> we profiled our initial lead molecule in a Cerep diversity profile. Thus, compound 6 was tested at a concentration of 10  $\mu$ M versus a panel of 69 receptors and ion channels and 14 enzymes (see complete list in the Supporting Information). Affinity for each target is measured by displacement of a radiolabeled ligand specific for each particular receptor or enzyme. The results, expressed in terms of percentage of displaced ligand, confirmed a notably clean profile for 6: in fact, for just 1 (norepinephrine transporter) out of 83 assessed targets was found a displacement higher than 50%. These initial results, positive in terms of mechanism of action and selectivity, encouraged us in further developing this class.

After the initial round of class expansion, compound 22 was selected for wider biological characterization. Prompted by the presence of an  $\alpha,\beta$ -unsaturated amide group in the structure, the electrophilic behavior of compound 22 was first examined. The compound was incubated at a test concentration of 100  $\mu$ M with glutathione (100  $\mu$ M) or *N*-acetyl-cysteine (100  $\mu$ M) at 25 °C. HPLC analysis carried out after 24 h incubation showed quantitative recovery of 22 without detection of any thiol adducts (see Supporting Information).

A more extensive assessment of the potency in the CRC assay was then carried out in comparison to the standard CsA. The CRC of freshly prepared mouse liver mitochondria was determined for 22 and CsA in a dose escalation series from 0.1 to 5.0  $\mu$ M (Figure 5). A clear dose response was observed with 22 and the compound enabled mitochondria to withstand very high levels of Ca<sup>2+</sup>, significantly superior to CsA. In addition, the CRC of CsA reached a plateau around 0.5  $\mu$ M of CsA and did not increase at higher doses. This is probably due the titration of cyclophilin D, its primary mitochondrial target.

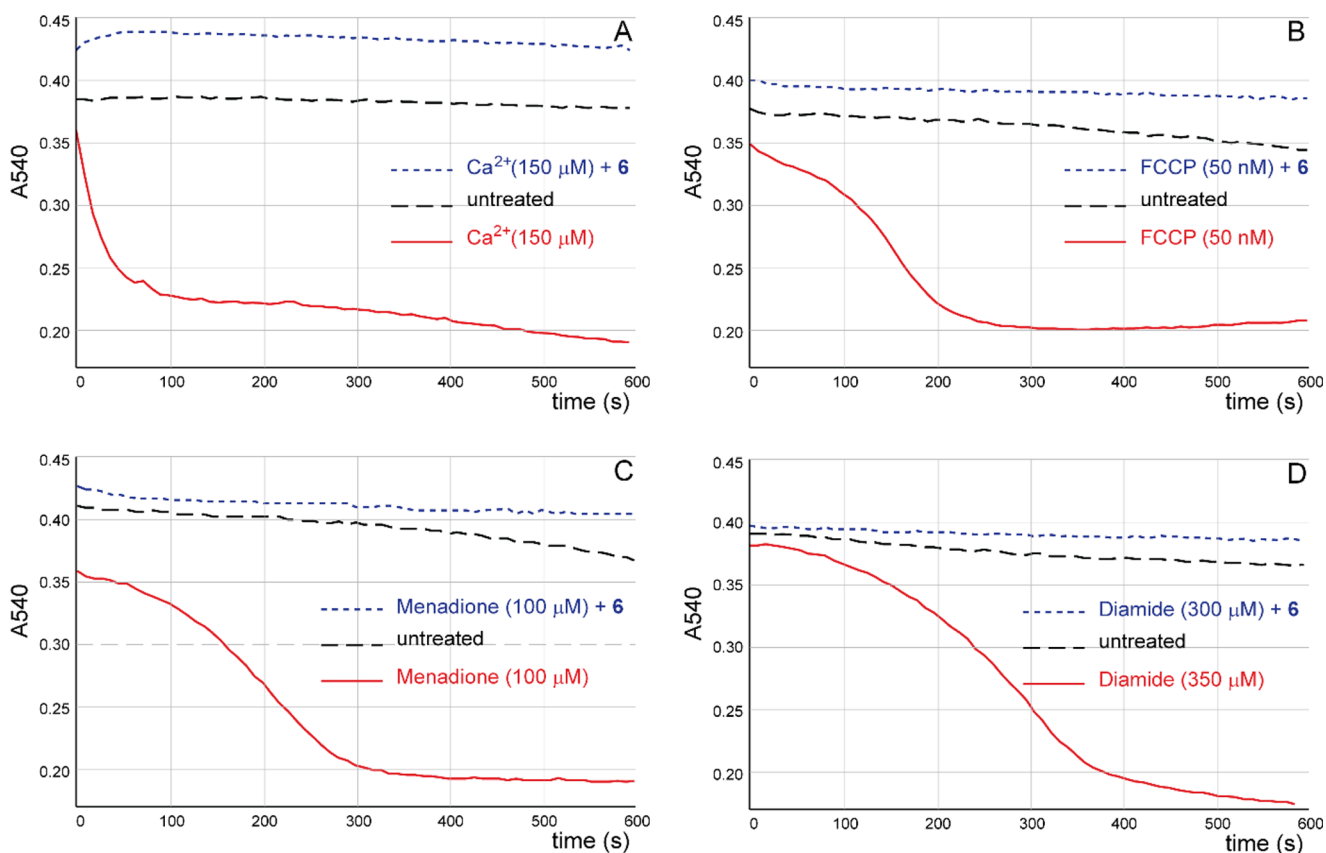


**Figure 4.** The cinnamic anilides inhibit opening of the mPTP in isolated mitochondria in response to various stimuli. Compound 6 (1 μM) inhibits swelling of mouse liver mitochondria exposed to (A) calcium overload (CaCl<sub>2</sub>, 150 μM), (B) uncoupling of electron transport chain (FCCP 50 nM), (C,D) oxidative stress (menadione 100 μM and diamide 300 μM, respectively).

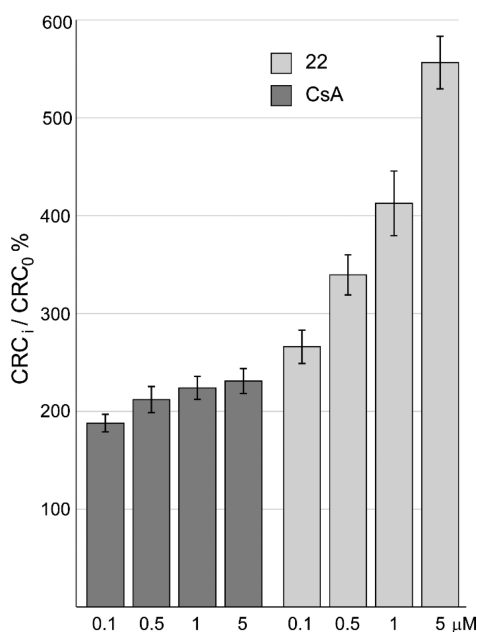


**Figure 5.** CRC of mouse liver mitochondria treated with increasing concentrations of 22 or CsA.

The observation that the CRC of CsA reached a plateau at relatively low concentrations while the cinnamic anilides continued to increase the CRC was the first indication that the molecular target of this new class might not be cyclophilin D. To further investigate this point, we measured the CRC of

CsA in combination with our inhibitors. Figure 6 shows that there is a clear additivity between CsA and 22. The protective effect of the combination is significantly higher than the maximum effect obtainable with CsA alone, which further confirms the hypothesis that the cinnamic anilides do not target cyclophilin D.

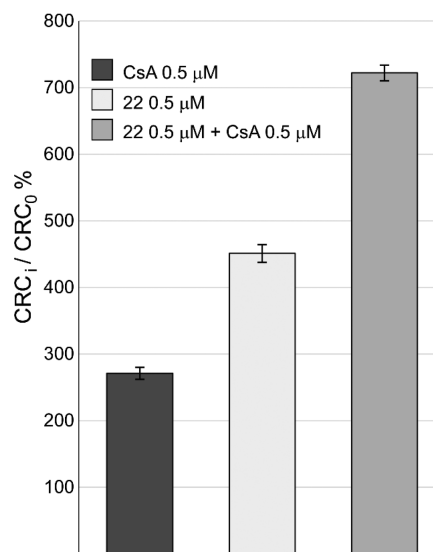


**Figure 6.** CRC of mouse liver mitochondria treated with combination of 22 and CsA; the results are the mean of three experiments ± standard deviation.

The potential use of mPTP inhibitors in preventing LRI after PCI requires that the inhibitor can reach the cardiac mitochondria very rapidly due to the fact that the mPTP opens within the first few minutes of reperfusion. To this end, we assessed the CRC of cardiac mitochondria after whole hearts had been perfused with the compound for just 2 min. Freshly prepared beating mouse hearts, immobilized on a Langendorff reperfusion apparatus, were perfused with compound **22** at a 5  $\mu\text{M}$  concentration or the corresponding amount of DMSO for 2 min. Hearts were then flushed with buffer, the mitochondria prepared, and the CRC measured (Figure 7A).

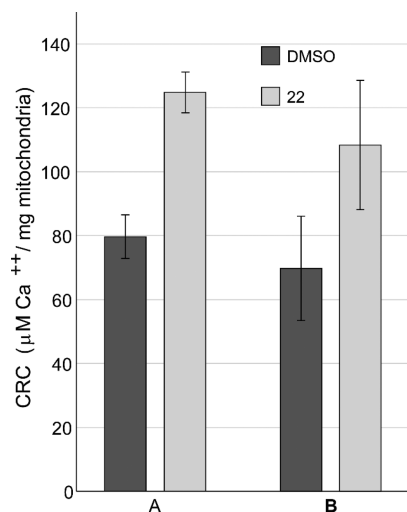


**Figure 7.** (A) Calcium retention capacity of mitochondria isolated from mouse hearts after perfusion with compound **22** (Langendorff apparatus) at 5  $\mu\text{M}$  for 2 min. Data expressed as absolute quantity of calcium retained. Vehicle (DMSO) treated group CRC = 80  $\mu\text{M}$ , SD = 6.8,  $n = 6$ ; treated group CRC = 125  $\mu\text{M}$ , SD = 6.0 ( $n = 6$ );  $p < 0.01$ . (B) Calcium retention capacity of mitochondria isolated from mouse hearts after 5 min from iv administration of compound **22** (15 mg/kg). Data expressed as absolute quantity of calcium retained. Vehicle (DMSO) treated group CRC = 69.8  $\mu\text{M}$ , SD = 15.7,  $n = 16$ ; treated group CRC = 108.4  $\mu\text{M}$ , SD = 20.2 ( $n = 6$ );  $p < 0.01$ .

Mitochondria from hearts perfused with **22** showed a significantly higher CRC than those treated with the vehicle (DMSO). These data clearly show that **22** can reach the cardiac mitochondria in whole organs in as little as 2 min.

Further, similar CRC experiments performed ex vivo on cardiac mitochondria prepared 5 min after iv injection of **22** (15 mg/kg) into the tail vein of mice confirmed that the compound, after systemic administration, is able to reach rapidly cardiac mitochondria and exert its protecting effect (Figure 7B).

On the basis of these results, we decided to assess the efficacy of **22** in a rabbit model of acute myocardial infarction.

New Zealand white rabbits were subjected to 30 min of left anterior descending (LAD) coronary artery ligation followed by 4 h of reperfusion. Animals were then sacrificed, and the hearts were analyzed to determine the area that had been ischemic (area at risk, AAR) during the ligation and the area that was necrotic (infarct size, IS) at the end of the reperfusion period. Animals were given either vehicle, **22**, or CsA via iv bolus injection 5 min prior to unligation of the LAD coronary artery. The ratio of the area at risk to infarct area (AAR/IS) is a measure of the extent of the final damage to the heart with

respect to the amount of tissue exposed to the ischemic insult. To correlate the pharmacodynamics response with plasma concentration of **22**, a satellite group of animals ( $n = 5$ ) was treated with the same dose of **22** and the test item quantified in plasma up to 240 min.

The data in Figure 8 clearly show that **22**, when given just prior to organ reperfusion, is cardioprotective in this animal

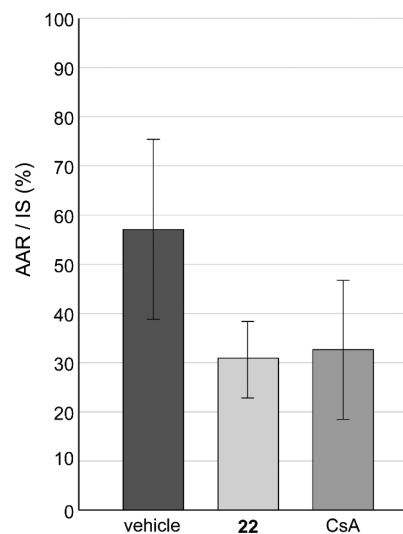


**Figure 8.** Compound **22** is cardioprotective in a rabbit model of acute myocardial infarction. Rabbits were subjected to left anterior descending (LAD) coronary artery occlusion for 30 min followed by 4 h of reperfusion. Compound **22** (5 mg/kg in 20% DMSO, 40% PEG400) and CsA (10 mg/kg as Sandimmune) were administered by iv bolus 5 min prior to reperfusion. Infarct size (IS) and area at risk (AAR) were determined by measuring TTC and Evans blue-stained heart slices. Vehicle treated group AAR/IS = 57.3%, SD = 18.1  $n = 8$ ; compound **22** treated group AAR/IS = 30.9%, SD = 7.8 ( $n = 8$ )  $p < 0.01$ ; CsA treated group AAR/IS = 32.6%, SD = 14.1 ( $n = 8$ )  $p < 0.01$ .

model of acute myocardial infarction and can reduce infarct size by almost 50%. Compound **22** showed a plasma concentration after 5 min of 4.8  $\mu\text{M}$  that reduced to 0.02  $\mu\text{M}$  after 240 min from the iv injection. The compound was cleared very rapidly in rabbit plasma, showing a  $t_{1/2}$  of about 30 min. However, as expected for an agent targeting I/R injury, this short-termed plasma exposure was able to induce a significant pharmacodynamic effect in this model of acute myocardial infarction. Further, the reduction in infarct size was similar to that seen with CsA, which works primarily by attenuating the mPTP, thus confirming the validity of targeting the mPTP.

Finally, to exclude potential cardiovascular side effects that could hamper the development of these compounds as novel therapeutics to treat acute ischemia-reperfusion injury, compound **22** was tested in vitro on the cardiac hERG channel and in vivo in a standard rat telemetry study. Compound **22** did not show any significant binding to hERG up to the concentration of 30  $\mu\text{M}$ , while no significant alterations of any of the monitored parameters (body temperature, heart rate, systolic and diastolic blood pressure) were observed in the rat safety study up to a dose of 30 mg/kg given iv, which correspond to plasma levels well above those observed in the efficacy experiments (see Supporting Information).

Taken together, these experiments strongly support the notion that administration of our cinnamic anilide mPTP

inhibitors during acute myocardial infarction and just prior to reperfusion therapy should prevent mPTP opening, attenuate lethal reperfusion injury, and reduce infarct size. Indeed, a drug candidate from this chemical series is currently undergoing clinical evaluation for the eventual treatment of lethal reperfusion injury in the setting of acute myocardial infarction.

## CONCLUSIONS

We identified a series of novel mPTP inhibitors based on the cinnamic anilido scaffold that are characterized by simplicity in structure, low molecular weight, and mechanism of action different from cyclophilin D inhibition.

On the basis of initial SAR studies, we identified the following structural requirements to gain mPTP inhibitory activity: (i) a phenol moiety at position 3 of the cinnamic phenyl ring, (ii) an unsubstituted acrylamido linker joining the cinnamic phenyl ring and the anilinic aryl moiety.

The high potential of cinnamic anilides is exemplified by the rapid identification of compound **22**, which demonstrated potency equal or higher than the gold standard, CsA, in a series of in vitro and in vivo experiments.

Taken together, all these findings highlight that this series of cinnamic anilides offer the possibility of studying the biology of the mPTP and the therapeutic potential of mPTP inhibition using potent, low molecular weight inhibitors.

## EXPERIMENTAL SECTION

Reagents and solvents used, unless stated otherwise, were of commercially available reagent grade quality and were used without further purification. Flash chromatography purifications were performed on Merck silica gel 60 (0.04–0.063 mm). Nuclear magnetic resonance spectra ( $^1\text{H}$  NMR) were recorded on a Bruker 400 MHz spectrometer at 300 K and are referenced in ppm ( $\delta$ ) relative to TMS. Coupling constants ( $J$ ) are expressed in hertz (Hz). HPLC–MS experiments were performed either on an Acquity UPLC apparatus, equipped with a diode array and a Micromass SQD single quadrupole (Waters) or on an Agilent 1100, equipped with a diode array and a Bruker ion–trap Esquire 3000+. Purity was monitored at 254 nm, and the purities of the compounds used for biological tests were found to be at least 95% with the exception of **10** (90%) and **11** (90%) (see Supporting Information).

**3-Acetoxy-4-hydroxycinnamic Acid (1n).** NaH (60%; 4.5 g, 113.29 mmol) was added portionwise to a solution of 3-hydroxy-4-methoxycinnamic acid (**10** g, 51.5 mmol) in dry THF (220 mL) while stirring at 0 °C under a nitrogen atmosphere. Stirring was continued at 0 °C for about 40 min, then acetic anhydride (7.3 mL, 77.25 mmol) was added dropwise at 0 °C. The reaction mixture was heated at reflux for about 3 h, further acetic anhydride (1.46 mL, 15.4 mmol) was added, and heating continued for additional 6 h. After cooling to rt, solvents were evaporated; the residue was taken up in 2 N HCl and water, extracted with EtOAc. The combined organic layers were washed with water and brine, dried over sodium sulfate, and concentrated to dryness. The resulting colorless powder was triturated in EtOAc, filtered, and dried under vacuum at 40 °C to afford 3-acetoxy-4-hydroxycinnamic acid **1n** (10 g, 82%) as a colorless powder.  $^1\text{H}$  NMR (500 MHz, DMSO- $d_6$ )  $\delta$  12.27 (s, 1H), 7.58–7.55 (m, 1H), 7.54–7.49 (m, 2H), 7.15 (m, 1H), 6.40 (d,  $J$  = 16.1 Hz, 1H), 3.81 (s, 3H), 2.26 (s, 3H).  $m/z$  (ES+), (M + Na) $^+$  = 259.

**(E)-N-(3-Chlorophenyl)-3-(3,4-dihydroxyphenyl)-prop-2-enamide (3).** 3-Chloroaniline **2a** (23.6  $\mu\text{L}$ , 2.22 mmol) and  $N,N'$ -dicyclohexylcarbodiimide (504 mg, 2.44 mmol) were added to a solution of caffeic acid **1a** (400 mg, 2.22 mmol) in THF (10 mL), and the resulting mixture was stirred at reflux for 7 h. After cooling to room temperature, the solid residue was filtered off and the remaining solution was evaporated. The residue was purified by flash silica chromatography (elution gradient: 20–50% EtOAc in *n*-hexane) to afford (E)-N-(3-chlorophenyl)-3-(3,4-dihydroxyphenyl)-prop-2-enam-

ide **3** (270 mg 48%) as a white powder.  $^1\text{H}$  NMR (400 MHz, DMSO- $d_6$ )  $\delta$  10.27 (bs, 1H), 9.38 (bs, 2H), 7.96 (m, 1H), 7.54 (m, 1H), 7.46 (d,  $J$  = 15.6 Hz, 1H), 7.38 (m, 1H), 7.14 (m, 1H), 7.05 (m, 1H), 6.96 (m, 1H), 6.82 (m, 1H), 6.54 (d,  $J$  = 15.6 Hz, 1H).  $m/z$  (ES+), (M + H) $^+$  = 290.

**(E)-N-(3-Chlorophenyl)-3-(3-hydroxyphenyl)-prop-2-enamide (4).** A solution of 3-hydroxycinnamic acid **1b** (1.0 g, 6.1 mmol) and thionyl chloride (0.53 mL, 7.32 mmol) in dry THF (15 mL) was stirred at 55 °C for 3 h. Then a further aliquot of thionyl chloride (0.1 mL, 1.38 mmol) was added, and the mixture was stirred at reflux temperature for additional 1.5 h. After cooling to about 5 °C, a solution of 3-chloroaniline **2a** (0.65 mL, 6.1 mmol) and triethylamine (3.4 mL, 24.4 mmol) in dry THF (5 mL) was added dropwise. After stirring at rt for 16 h, the reaction mixture was diluted with DCM and washed with water, 0.5N aqueous hydrochloric acid, and brine. Organic layer was dried over sodium sulfate, concentrated under reduced pressure, and purified by flash silica chromatography (petroleum ether/EtOAc 45:55) to afford (E)-N-(3-chlorophenyl)-3-(3-hydroxyphenyl)-prop-2-enamide **4** (671 mg, 40%) as a beige solid.  $^1\text{H}$  NMR (400 MHz, DMSO- $d_6$ )  $\delta$  10.37 (s, 1H), 9.64 (s, 1H), 7.93 (m, 1H), 7.53–7.49 (m, 2H), 7.37 (m, 1H), 7.25 (m, 1H), 7.13 (m, 1H), 7.05 (m, 1H), 6.70 (m, 1H), 6.83 (m, 1H), 6.72 (d,  $J$  = 15.6 Hz, 1H).  $m/z$  (ES+), (M + H) $^+$  = 274.

**(E)-3-(3-Aminophenyl)-N-(3-chlorophenyl)-prop-2-enamide (10).**  $\text{SnCl}_4 \cdot 2\text{H}_2\text{O}$  (530 mg, 2.35 mmol) was added to a solution of (E)-3-(3-nitrophenyl)-N-(3-chlorophenyl)-prop-2-enamide **10a** (142 mg, 0.47 mmol) in EtOH/EtOAc 1/1 (6 mL). After stirring at reflux for 7 h, the reaction mixture was cooled to rt and poured onto ice/water; pH was adjusted to 8 with  $\text{NaHCO}_3$  (satd aq), and the resulting aqueous solution was extracted with ethyl acetate. The combined organic layers were washed with brine, dried over sodium sulfate, and concentrated under reduced pressure to afford (E)-3-(3-aminophenyl)-N-(3-chlorophenyl)-prop-2-enamide **10** (88 mg, 69%) as an orange solid.  $^1\text{H}$  NMR (400 MHz, DMSO- $d_6$ )  $\delta$  10.37 (s, 1H), 7.94 (m, 1H), 7.52 (m, 1H), 7.44 (d,  $J$  = 15.67 Hz, 1H), 7.36 (m, 1H), 7.14–7.07 (m, 2H), 6.78–6.75 (m, 2H), 6.66 (d,  $J$  = 15.67 Hz, 1H), 6.61 (m, 1H), 5.25 (s, 2H).  $m/z$  (ES+), (M + H) $^+$  = 273.

**(E)-N-(3-Chlorophenyl)-3-[3-[(methylsulfonyl)amino]phenyl]-prop-2-enamide (11).** A solution of 3-[(methylsulfonyl)amino]cinnamic acid **1i** (329 mg, 1.36 mmol), oxalyl chloride (0.35 mL, 4.1 mmol), and catalytic dry DMF in dry DCM (15 mL) was stirred at reflux for 1.5 h. After cooling to rt, solvent and excess oxalyl chloride were evaporated under reduced pressure and the residue was taken up in dry toluene and concentrated. A solution of 3-chloroaniline **2a** (0.144 mL, 1.36 mmol) and triethylamine (0.284 mL, 2.04 mmol) in dry DCM (8 mL) was added dropwise at 0 °C to the raw acyl chloride in toluene. After stirring at rt for 16 h, the reaction mixture was diluted with DCM and washed with water, 0.5N aqueous hydrochloric acid,  $\text{NaHCO}_3$  (satd aq), and brine. Organic layer was dried over sodium sulfate, concentrated under reduced pressure, and purified by flash silica chromatography (DCM/acetone 97:3) and trituration with diisopropyl ether/methanol to afford (E)-N-(3-chlorophenyl)-3-[3-[(methylsulfonyl)amino]phenyl]-prop-2-enamide **11** (50 mg, 14%) as a beige solid.  $^1\text{H}$  NMR (400 MHz, DMSO- $d_6$ )  $\delta$  11.5 (s, 1H), 9.92 (s, 1H), 7.94 (m,bs, 1H), 7.60–7.34 (m, 6H), 7.25–7.12 (m, 2H), 6.77 (d,  $J$  = 15.65 Hz, 1H), 3.35 (s, 3H).  $m/z$  (ES+), (M + H) $^+$  = 351.

**(E)-N-(3-Chlorophenyl)-3-(1H-indol-6-yl)-prop-2-enamide (12).** EDC hydrochloride (245 mg, 1.28 mmol) and HOBt (173 mg, 1.28 mmol) were added to a solution of (E)-3-(1H-indol-6-yl)-prop-2-enoic acid **1j** (120 mg, 0.64 mmol) in dry DCM (6 mL) while cooling at 0 °C. The mixture was allowed to warm to room temperature and stirred for 45 min. 3-Chloroaniline **2a** (0.082 mL, 0.77 mmol) was added, and the mixture was stirred at room temperature for 4 h, then at reflux for 7 h. After cooling, the mixture was diluted with DCM, washed with  $\text{NaHCO}_3$  (satd aq), dried over sodium sulfate, filtered, and concentrated. The residue was purified by flash silica chromatography (elution gradient: DCM/MeOH 100:0.5) to afford (E)-N-(3-chlorophenyl)-3-(1H-indol-6-yl)-prop-2-enamide **12** (82 mg, 43%) as a pale-yellow powder.  $^1\text{H}$  NMR (400 MHz, DMSO- $d_6$ )

$\delta$  11.35 (s, 1H), 10.30 (s, 1H), 7.95 (t,  $J = 2$ , 1H), 7.70 (d,  $J = 15.6$ , 1H), 7.64 (s, 1H), 7.59 (d,  $J = 8.4$ , 1H), 7.54–7.52 (m, 1H), 7.46 (t,  $J = 2.6$ , 1H), 7.36 (t,  $J = 8$ , 1H), 7.30 (dd,  $J = 8.4$ ,  $J = 1.2$ , 1H), 7.11 (dd,  $J = 8$ ,  $J = 1.2$ , 1H), 6.75 (d,  $J = 15.6$ , 1H), 6.47 (m, 1H).  $m/z$  (ES+),  $(2M + Na)^+ = 615$ .

**(E)-N-(3-Chlorophenyl)-3-(4-amino-3-hydroxyphenyl)-prop-2-enamide (14).** SnCl<sub>2</sub>·2H<sub>2</sub>O (562 mg, 2.5 mmol) was added to a solution of (E)-N-(3-chlorophenyl)-3-(3-hydroxy-4-nitrophenyl)-prop-2-enamide **14a** (159 mg, 0.5 mmol) in EtOH (6 mL). The mixture was stirred at reflux for about 1.5 h, cooled to room temperature, and concentrated. The residue was taken up with NaHCO<sub>3</sub> (satd aq) and Rochelle's salt solution and extracted with EtOAc. The combined organic layers were washed with brine, dried over sodium sulfate, and concentrated under reduced pressure to afford (E)-N-(3-chlorophenyl)-3-(4-amino-3-hydroxyphenyl)-prop-2-enamide **14** (89 mg, 62%) as a yellow powder. <sup>1</sup>H NMR (400 MHz, DMSO-*d*<sub>6</sub>)  $\delta$  10.16 (s, 1H), 9.34 (s, 1H), 7.93 (t,  $J = 1.6$  Hz, 1H), 7.50 (m, 1H), 7.34 (m, 2H), 7.08 (m, 1H), 6.92 (s, 1H), 6.87 (m, 1H), 6.59 (d,  $J = 8.0$  Hz, 1H), 6.38 (t,  $J = 15.6$  Hz, 1H), 5.15 (s, 2H).  $m/z$  (ES+),  $(M + H)^+ = 289$ .

**(E)-N-(3-Aminophenyl)-3-(3-hydroxy-4-methoxyphenyl)-prop-2-enamide (18).** A suspension of (E)-3-(3-hydroxy-4-methoxyphenyl)-N-(3-nitrophenyl)-prop-2-enamide **18a** (314 mg, 1.00 mmol) and SnCl<sub>2</sub>·2H<sub>2</sub>O (1.128 g, 5.00 mmol) in EtOH (20 mL) was heated at reflux for 1.5 h. The resulting solution was cooled to room temperature and concentrated. The residue was taken up with NaHCO<sub>3</sub> (satd aq) and Rochelle's salt solution and extracted with EtOAc. The combined organic layers were dried over sodium sulfate, filtered, and concentrated. Purification by flash silica chromatography (DCM/MeOH 98:2) afforded (E)-N-(3-aminophenyl)-3-(3-hydroxy-4-methoxyphenyl)-prop-2-enamide **18** (110 mg, 39%) as an off-white powder. <sup>1</sup>H NMR (400 MHz, DMSO-*d*<sub>6</sub>)  $\delta$  9.75 (s, 1H), 9.19 (s, 1H), 7.38 (d,  $J = 15.6$  Hz, 1H), 7.02–6.90 (m, 5H), 6.79 (d,  $J = 8.0$  Hz, 1H), 6.60 (d,  $J = 15.6$  Hz, 1H), 6.26 (dd,  $J = 8.0$  Hz,  $J = 1.2$  Hz, 1H), 5.05 (s, 2H), 3.81 (s, 3H).  $m/z$  (ES+),  $(2M + Na)^+ = 591$ .

**(E)-N-(3-Carboxamidophenyl)-3-(3-acetoxy-4-methoxyphenyl)prop-2-enamide (24a).** A solution of 3-acetoxy-4-methoxycinnamic acid **1n** (0.45 g, 1.9 mmol), thionyl chloride (0.14 mL, 2.66 mmol), and 3 drops of DMF in dry THF (10 mL) was stirred at reflux for 2 h. Then a further aliquot of thionyl chloride (0.05 mL, 0.76 mmol) was added, and the mixture was stirred at reflux temperature for additional 2 h. After cooling to about 5 °C, a solution of 3-aminobenzamide **2j** (0.259 g, 1.9 mmol) and triethylamine (0.53 mL, 3.8 mmol) in dry DCM (5 mL) was added dropwise. After stirring at rt overnight, THF was removed under vacuum and the residue was triturated in DCM to give a first aliquot of the target cinnamic anilide **24a** as a beige solid (185 mg). After filtration, the solution was washed with 1N aqueous hydrochloric acid and NaHCO<sub>3</sub> (satd aq), dried over sodium sulfate, and evaporated to afford a second aliquot of **24a**. The two solids were mixed and triturated in DCM to yield (E)-N-(3-carboxamidophenyl)-3-(3-acetoxy-4-methoxyphenyl)prop-2-enamide **24a** (671 mg, 79%).  $m/z$  (ES+),  $(M + Na)^+ = 377$ .

**(E)-N-(3-Carboxamidophenyl)-3-(3-hydroxy-4-methoxyphenyl)prop-2-enamide (24).** A suspension of (E)-N-(3-carboxamidophenyl)-3-(3-acetoxy-4-methoxyphenyl)prop-2-enamide **24a** (535 mg, 1.5 mmol) and NaOH (50% in water) (0.16 mL, 3 mmol) in MeOH (5 mL) was stirred at reflux for 1 h. After cooling to room temperature, MeOH was evaporated, the reaction mixture was diluted with water, and pH was adjusted to 6 with 2 N HCl. The resulting precipitate was filtered off, washed with water, and dried under vacuum to afford (E)-N-(3-carboxamidophenyl)-3-(3-hydroxy-4-methoxyphenyl)prop-2-enamide **24** (252 mg, 54%) as a white solid. <sup>1</sup>H NMR (400 MHz, DMSO-*d*<sub>6</sub>)  $\delta$  10.21 (s, 1H), 9.23 (s, 1H), 8.10 (s, 1H), 7.92–7.87 (m, 2H), 7.54 (d,  $J = 7.6$  Hz, 1H), 7.45 (d,  $J = 15.6$  Hz, 1H), 7.39 (t,  $J = 8.0$  Hz, 1H), 7.32 (s, 1H), 7.05–7.03 (m, 2H), 6.97 (d,  $J = 8.4$  Hz, 1H), 6.60 (d,  $J = 15.6$  Hz, 1H), 3.81 (s, 3H).  $m/z$  (ES+),  $(2M + H)^+ = 625$ .

**(E)-3-(3-Hydroxy-4-methoxyphenyl)-N-indan-1-yl-acrylamide (28).** (E)-3-(3-Acetoxy-4-methoxyphenyl)-N-indan-1-yl-acrylamide **28a** (267 mg, 0.76 mmol) was treated with 3 N HCl in MeOH

(5 mL, 1.67 mmol), at room temperature for about 1.5 h. Solvents were evaporated, and the residue was taken up in MeOH and concentrated (twice), then triturated with diethyl ether and filtered to give (E)-3-(3-hydroxy-4-methoxyphenyl)-N-indan-1-yl-acrylamide **28** (237 mg, 100%) as a green powder. <sup>1</sup>H NMR (400 MHz, DMSO-*d*<sub>6</sub>)  $\delta$  8.39 (m, 1H), 7.35 (d,  $J = 15.6$  Hz, 1H), 7.27–7.17 (m, 4H), 6.98–6.93 (m, 3H), 6.44 (d,  $J = 16.0$  Hz, 1H), 5.39 (q,  $J = 7.6$  Hz, 1H), 3.79 (s, 3H), 2.99–2.92 (m, 1H), 2.86–2.78 (m, 1H), 2.47–2.39 (m, 1H), 1.86–1.80 (m, 1H).  $m/z$  (ES+),  $(2M + Na)^+ = 641$ .

**(E)-3-(3-Hydroxy-4-methoxyphenyl)-N-(2-naphthyl)-prop-2-enamide (29).** K<sub>2</sub>CO<sub>3</sub> (61.4 mg, 0.44 mmol) was added to a solution of (E)-3-(3-acetoxy-4-methoxyphenyl)-N-(2-naphthyl)-prop-2-enamide **29a** (80 mg, 0.22 mmol) in MeOH:THF:water 10:1:1 (4.8 mL). After stirring for 2 h at rt, solvents were evaporated, the residue was partitioned between EtOAc, and water and the aqueous phase was extracted with EtOAc. The combined organic layers were dried over sodium sulfate, filtered, and concentrated to dryness to afford (E)-3-(3-hydroxy-4-methoxyphenyl)-N-(2-naphthyl)-prop-2-enamide **29** (70 mg, 100%) as a yellow powder. <sup>1</sup>H NMR (500 MHz, DMSO-*d*<sub>6</sub>)  $\delta$  10.39 (s, 1H), 9.02–8.97 (m, 1H), 8.41 (s, 1H), 7.91–7.77 (m, 3H), 7.72–7.64 (m, 1H), 7.43–7.42 (m, 1H), 7.50–7.32 (m, 3H), 7.09–7.03 (m, 1H), 7.00–6.88 (m, 2H), 6.66 (d,  $J = 15.7$  Hz, 1H), 3.80 (s, 3H).  $m/z$  (ES+),  $(M + H)^+ = 318$ .

**(E)-N-Benzoxazol-4-yl-3-(3-acetoxy-4-methoxyphenyl)prop-2-enamide (31a).** A solution of 3-acetoxy-4-hydroxycinnamic acid **1n** (236 mg, 1 mmol) and thionyl chloride (0.09 mL, 1.2 mmol) in dry THF (5 mL) was stirred at 55 °C for 3 h. Then a further aliquot of thionyl chloride (0.07 mL, 1 mmol) was added, and the mixture was stirred at reflux for additional 2 h. After cooling to rt, solvents were evaporated, and dry THF (3 mL) was added, followed by a solution of 4-amino-benzoxazole **2q** (168 mg, 1.25 mmol) and triethylamine (0.42 mL, 3 mmol) in dry THF (2 mL). After stirring at rt for 2 h, solvent was evaporated, and the residue was taken up in EtOAc and washed with water, NaHCO<sub>3</sub> (satd aq), and brine. The organic layer was dried over sodium sulfate, filtered, and evaporated. The residue was triturated in acetone and then DCM to afford (E)-N-benzoxazol-4-yl-3-(3-acetoxy-4-methoxyphenyl)prop-2-enamide **31a** (66 mg, 19%) as a light-yellow powder. <sup>1</sup>H NMR (500 MHz, DMSO-*d*<sub>6</sub>)  $\delta$  2.28 (s, 3H) 3.82 (s, 3H) 7.11–8.34 (m, 8H) 8.79 (s, 1H) 10.26 (s, 1H).  $m/z$  (ES+),  $(M + H)^+ = 353$ .

**(E)-3-(3-Hydroxy-4-methoxyphenyl)-N-(1-methyl-1H-indazol-4-yl)prop-2-enamide hydrochloride (32).** A solution of 3-acetoxy-4-hydroxycinnamic acid **1n** (236 mg, 1 mmol) and thionyl chloride (0.08 mL, 1.1 mmol) in dry THF (5 mL) was stirred at 55 °C for 2 h. Then a further aliquot of thionyl chloride (0.03 mL, 0.4 mmol) was added, and the mixture was stirred at reflux for additional 2 h. After cooling to rt, a solution of 4-amino-1-methyl-indazole **2r** (147 mg, 1 mmol) and triethylamine (0.42 mL, 3 mmol) in dry THF (2 mL) was added dropwise. After stirring at rt for 22 h, solvent was evaporated, and the residue was taken up in EtOAc and washed with water, NaHCO<sub>3</sub> (satd aq), and brine. The organic layer was dried over sodium sulfate, concentrated under reduced pressure, and purified by flash silica chromatography (DCM/EtOAc 90:10), followed by trituration with diethyl ether. The resulting solid (30 mg, 0.08 mmol) was suspended in 3 N HCl in MeOH (2 mL) and stirred at rt for 2 h. Solvents were evaporated, and the residue was taken up in MeOH and concentrated (twice) and finally triturated in diethyl ether to afford (E)-3-(3-hydroxy-4-methoxyphenyl)-N-(1-methyl-1H-indazol-4-yl)prop-2-enamide hydrochloride **32** (20 mg, 6%) as a beige powder. <sup>1</sup>H NMR (400 MHz, DMSO-*d*<sub>6</sub>)  $\delta$  10.10 (s, 1H), 9.24 (s, 1H), 8.31 (s, 1H), 7.88 (m, 1H), 7.50 (d,  $J = 15.6$  Hz, 1H), 7.37–7.32 (m, 2H), 7.09–7.06 (m, 2H), 6.99 (d,  $J = 8.0$  Hz, 1H), 6.86 (d,  $J = 15.6$  Hz, 1H), 4.03 (s, 3H), 3.82 (s, 3H).  $m/z$  (ES+),  $(M + H)^+ = 324$ .

**(E)-3-(3-Hydroxy-4-methoxyphenyl)-N-methoxy-N-methylprop-2-enamide (35).** *N,O*-Dimethylhydroxylamine hydrochloride (1.2 g, 12.4 mmol), EDC hydrochloride (2.38 g, 12.4 mmol), and HOBt (837 mg, 6.2 mmol) were added to a suspension of 3-hydroxy-4-methoxycinnamic acid **1d** (2 g, 10.3 mmol) in DCM (10 mL). After stirring at room temperature for 16 h, the reaction mixture was diluted with DCM and washed with water. Purification by flash silica

chromatography (*n*-hexane/EtOAc 1:1) afforded (*E*)-3-(3-hydroxy-4-methoxyphenyl)-*N*-methoxy-*N*-methyl-prop-2-enamide **35** (607 mg, 25%) as an off-white powder. <sup>1</sup>H NMR (400 MHz, CDCl<sub>3</sub>) δ 7.66 (d, 1H, *J* = 15.7), 7.23 (d, 1H, *J* = 2.1), 7.07 (dd, 1H, *J* = 8.3, 2.1), 6.91 (d, 1H, *J* = 15.7), 6.86 (d, 1H, *J* = 8.3), 3.94 (s, 3H), 3.78 (s, 3H), 3.32 (s, 3H). *m/z* (ES<sup>+</sup>), (*M* + H)<sup>+</sup> = 238.

**trans-rac-N-Methoxy-N-methyl-2-(3-hydroxy-4-methoxyphenyl)cyclopropanecarboxamide (36).** DMSO (7 mL) was added dropwise to a mixture of NaH (274 mg, 6.88 mmol) and trimethylsulfoxonium iodide (1.5 g, 6.88 mmol). After stirring at room temperature for 30 min, a solution of (*E*)-3-(3-hydroxy-4-methoxyphenyl)-*N*-methoxy-*N*-methyl-prop-2-enamide **35** (407 mg, 1.72 mmol) in DMSO (3 mL) was added, and the resulting mixture was stirred overnight. The reaction mixture was poured into water, acidified to pH 3 with 2 N HCl, and extracted with diethyl ether. The combined organic layers were dried over sodium sulfate and concentrated under reduced pressure. Purification by flash silica chromatography afforded *trans-rac-N*-methoxy-*N*-methyl-2-(3-hydroxy-4-methoxyphenyl)cyclopropane-carboxamide **36** (331 mg, 77%) as an off-white powder. <sup>1</sup>H NMR (400 MHz, CDCl<sub>3</sub>) δ 6.79–6.69 (m, 3H), 3.89 (s, 3H), 3.72 (s, 3H), 3.25 (s, 3H), 2.48–2.41 (m, 1H), 2.36 (m, 1H), 1.62–1.58 (m, 2H), 1.28–1.25 (m, 1H). *m/z* (ES<sup>+</sup>), (*M* + H)<sup>+</sup> = 252.

**trans-rac-N-(3-Chlorophenyl)-2-(3-hydroxy-4-methoxyphenyl)cyclopropanecarboxamide (37).** To a suspension of *trans-rac-N*-methoxy-*N*-methyl-2-(3-hydroxy-4-methoxyphenyl)cyclopropane-carboxamide **36** (330 mg, 1.31 mmol) in diethyl ether (8 mL) was added *t*-BuOK (884 mg, 7.88 mmol) followed by water (47 mL). The reaction mixture was stirred for 20 h, then poured onto crushed ice and extracted twice with diethyl ether. The aqueous phase was cooled to 0 °C and acidified to pH 1 with 1 N HCl. Extraction with diethyl ether afforded raw *trans-rac*-2-(3-hydroxy-4-methoxyphenyl)cyclopropanecarboxylic acid as a yellow oil that was used in the next step without any further purification. 2-(3-Hydroxy-4-methoxyphenyl)cyclopropanecarboxylic (130 mg, 0.62 mmol), 3-chloroaniline **2a** (86 μL, 0.81 mmol), and a catalytic amount of HOBt were added to a suspension of EDC hydrochloride (144 mg, 0.75 mmol) in DCM (5 mL). The resulting mixture was stirred at room temperature for 36 h, poured into water, and the organic phase was washed twice with water, dried over sodium sulfate, filtered, and concentrated. Purification by flash silica chromatography (*n*-hexane/EtOAc 3:1) afforded *trans-rac-N*-(3-chlorophenyl)-2-(3-hydroxy-4-methoxyphenyl)cyclopropanecarboxamide **37** (57 mg, 29%) as an off-white powder. <sup>1</sup>H NMR (400 MHz, DMSO-*d*<sub>6</sub>) δ 10.39 (s, 1H), 8.90 (s, 1H), 7.83 (t, 1H, *J* = 2 Hz), 7.44–7.43 (m, 1H), 7.32 (m, 1H, *J* = 8.1 Hz), 7.10–7.07 (m, 1H), 6.83 (d, 1H, *J* = 8.1), 6.60–6.56 (m, 2H), 3.73 (s, 3H), 2.25 (m, 1H), 1.95 (m, 1H), 1.43 (m, 1H), 1.24 (m, 1H). *m/z* (ES<sup>+</sup>), (*M* + H)<sup>+</sup> = 318.

**N-(3-Chlorophenyl)carbamothioyl]-3-acetoxy-4-methoxybenzamide (40).** A solution of 3-acetoxy-4-methoxybenzoic acid **38** (0.5 g, 2.38 mmol), thionyl chloride (0.19 mL, 2.62 mmol), and 3 drops of DMF in dry THF (10 mL) was stirred at reflux for 2 h. The mixture was then concentrated in vacuo, treated twice with toluene, and dried. The crude was taken up with CH<sub>3</sub>CN (5 mL), KSCN (231 mg, 2.38 mmol) was added, and the resulting mixture was heated at reflux for additional 2 h. After cooling to room temperature, KCl was filtered off, 3-chloroaniline (225 μL, 2.14 mmol) in CH<sub>3</sub>CN (2 mL) was added, and the solution was stirred for 0.5 h at rt. Filtration of the resulting solid afforded *N*-[(3-chlorophenyl)carbamothioyl]-3-acetoxy-4-methoxybenzamide **40** (704 mg, 87%) as a white powder. <sup>1</sup>H NMR (300 MHz, DMSO-*d*<sub>6</sub>) δ 12.58 (br s, 1H), 11.49 (br s, 1H), 8.00 (dd, *J* = 8.6, 2.2 Hz, 1H), 7.95 (s, 1H), 7.84 (d, *J* = 2.3 Hz, 1H), 7.65–7.53 (m, 1H), 7.45 (t, *J* = 7.9, 1H), 7.33 (ddd, *J* = 7.9, 2.0, 0.9 Hz, 1H), 7.29 (d, *J* = 8.8 Hz, 1H), 3.89 (s, 3H), 2.30 (s, 3H). *m/z* (ES<sup>+</sup>), (*M* + H)<sup>+</sup> = 379.

**5-[5-(3-Chloroanilino)-4*H*-1,2,4-triazol-3-yl]-2-methoxyphenol (41).** A solution of *N*-[(3-chlorophenyl)carbamothioyl]-3-acetoxy-4-methoxybenzamide **40** (0.3 g, 0.79 mmol) and hydrazine hydrate (0.19 μL, 3.95 mmol) in CHCl<sub>3</sub> (8 mL) was stirred at reflux for 2 h. After cooling to room temperature, the resulting solid was filtered and

purified by flash silica chromatography (elution gradient: 2–5% MeOH in DCM) to afford 5-[5-(3-chloroanilino)-4*H*-1,2,4-triazol-3-yl]-2-methoxyphenol **41** (81 mg, 32%) as a white powder. <sup>1</sup>H NMR (400 MHz, DMSO-*d*<sub>6</sub>) δ 9.46 (s, 1H), 9.28 (br s, 1H), 7.76 (t, *J* = 2.05 Hz, 1H), 7.45 (dd, *J* = 8.22, 2.05 Hz, 1H), 7.36–7.42 (m, 2H), 7.24 (t, *J* = 8.07 Hz, 1H), 7.06 (d, *J* = 9.10 Hz, 1H), 6.83 (dd, *J* = 7.63, 1.47 Hz, 1H), 3.83 (s, 3H). *m/z* (ES<sup>+</sup>), (*M* + H)<sup>+</sup> = 317.

**5-[(*E*)-2-[5-(3-Chlorophenyl)-1,3,4-oxadiazol-2-yl]ethenyl]-2-methoxyphenyl acetate (43).** A mixture of 3-acetoxy-4-hydroxycinnamic acid **1n** (210 mg, 0.9 mmol), 3-chlorobenzoic acid hydrazide **42** (157.5 mg, 0.9 mmol), and POCl<sub>3</sub> (2.5 mL) was heated at reflux for 1 h. After cooling to rt, the reaction mixture was poured onto ice/water and extracted with EtOAc. The combined organic layers were washed with NaHCO<sub>3</sub> (satd aq) and brine, dried over sodium sulfate, filtered, and concentrated to dryness. Purification by flash silica chromatography (*n*-hexane/EtOAc 80:20) afforded 5-[(*E*)-2-[5-(3-chlorophenyl)-1,3,4-oxadiazol-2-yl]ethenyl]-2-methoxyphenyl acetate **43** (100 mg, 30%) as a colorless powder. <sup>1</sup>H NMR (500 MHz, DMSO-*d*<sub>6</sub>) δ 8.11 (m, 1H), 8.08–8.05 (m, 1H), 7.77 (d, *J* = 16.4 Hz, 1H), 7.75–7.65 (m, 4H), 7.28 (d, *J* = 16.4 Hz, 1H), 7.22 (m, 1H), 3.84 (s, 3H), 2.30 (s, 3H). *m/z* (ES<sup>+</sup>), (*M* + H)<sup>+</sup> = 371.

**5-[(*E*)-2-[5-(3-Chlorophenyl)-1,3,4-oxadiazol-2-yl]ethenyl]-2-methoxyphenol (44).** A solution of 5-[(*E*)-2-[5-(3-chlorophenyl)-1,3,4-oxadiazol-2-yl]ethenyl]-2-methoxyphenyl acetate **43** (100 mg, 0.27 mmol) in MeOH (2 mL) was treated with 4 N HCl in 1,4-dioxane (1.1 mL, 0.27 mmol) at rt for 6 h. Solvents were evaporated and the residue taken up in diethyl ether and filtered. Purification by flash silica chromatography (elution gradient: 10–25% acetone in *n*-hexane) afforded 5-[(*E*)-2-[5-(3-chlorophenyl)-1,3,4-oxadiazol-2-yl]ethenyl]-2-methoxyphenol **44** (20 mg, 22%) as a colorless powder. <sup>1</sup>H NMR (500 MHz, DMSO-*d*<sub>6</sub>) δ 9.21 (s, 1H), 8.13 (m, 1H), 8.07 (m, 1H), 7.74–7.64 (m, 3H), 7.22 (m, 2H), 7.09 (d, *J* = 16.4 Hz, 1H), 7.01 (m, 1H), 3.83 (s, 3H). *m/z* (ES<sup>+</sup>), (*M* + H)<sup>+</sup> = 329.

**N-(3-Chlorophenyl)-3-(3-hydroxy-4-methoxy-phenyl)propanamide (46).** A solution of 3-(3-hydroxy-4-methoxy-phenyl)propanoic acid (0.5 g, 2.57 mmol), thionyl chloride (0.2 mL, 2.83 mmol), and 3 drops of DMF in dry THF (15 mL) was stirred at reflux for 2 h. Then a further aliquot of thionyl chloride (50 μL, 0.69 mmol) was added, and the mixture was stirred at reflux temperature for additional 2 h. After cooling to about 5 °C, a solution of 3-Cl-aniline (0.27 mL, 2.57 mmol) and triethylamine (0.71 mL, 5.14 mmol) in dry DCM (5 mL) was added dropwise. After stirring at rt for 16 h, the reaction mixture was concentrated under vacuum, diluted with DCM, and washed with water, 0.5 N aqueous hydrochloric acid, and brine. Organic layer was dried over sodium sulfate, concentrated under reduced pressure, and purified by flash silica chromatography (hexane/EtOAc 6:4) to afford *N*-(3-chlorophenyl)-3-(3-hydroxy-4-methoxy-phenyl)propanamide **46** (430 mg, 55%) as an off-white powder. <sup>1</sup>H NMR (400 MHz, DMSO-*d*<sub>6</sub>) δ 10.05 (s, 1H), 8.79 (s, 1H), 7.81 (t, *J* = 2.0 Hz, 1H), 7.43–7.40 (m, 1H), 7.31 (t, *J* = 8.0 Hz, 1H), 7.09–7.06 (m, 1H), 6.80 (d, *J* = 8.0 Hz, 1H), 6.66 (d, *J* = 2.0 Hz, 1H), 6.60 (dd, *J* = 8.4 Hz, *J* = 2.0 Hz, 1H), 3.71 (s, 3H), 2.76 (t, *J* = 8.0 Hz, 2H), 2.55 (t, *J* = 8.0 Hz, 2H). *m/z* (ES<sup>+</sup>), (2*M* + Na)<sup>+</sup> = 633.

#### Induction of mPTP Opening in Isolated Mitochondria.

Mitochondria were freshly prepared from C57/bl6 male mouse livers as previously described.<sup>35</sup> Briefly, each mouse liver was excised after cervical dislocation and placed in ice-cold “mitochondria buffer” (250 mM sucrose, 10 mM Tris-HCl, 0.1 mM EGTA, pH 7.4). Liver was rinsed 3–4 times with ice-cold mitochondria buffer, minced with scissors, and passed through a 7 mL Dounce homogenizer (Wheaton) using three strokes with a “loose” pestle in ice. The homogenate was diluted to 50 mL and centrifuged at 900g for 10 min at 4 °C (Beckman Avanti J-25 refrigerated). The supernatant was carefully decanted and centrifuged at 7000g for 10 min at 4 °C. The mitochondrial pellet was carefully washed with 2 mL of ice-cold mitochondria buffer, diluted to 50 mL, and spun at 7000g for 10 min at 4 °C. The resulting mitochondrial pellet was resuspended in 500 μL of mitochondria buffer and stored in ice. Protein concentration was determined using the Biuret assay.

**Isolation of Mitochondria from Mouse Heart.** Hearts were minced with scissors (into very small pieces) in 3 mL of mitochondria buffer (250 mM Sucrose, 10 mM Tris-HCl, 0.1 mM EGTA, 0.1% BSA; pH 7.4) and homogenized with a 1 mL Dounce homogenizer (Wheaton) using four strokes of a “loose” pestle and two strokes of a “tight” pestle. The homogenates were centrifuged in 1.5 mL tubes at 3100 rpm (Heraeus Biofuge Fresco centrifuge) for 10 min at 4 °C. The supernatant was then centrifuged at 8700 rpm for 10 min, and the resulting pellet was washed with 1 mL of mitochondria buffer (without BSA) followed by another centrifugation at 8700 rpm for 10 min. Pellet was then resuspended in CRC buffer (see CRC assay description).

**Mitochondrial Swelling Assay.** For mitochondrial swelling experiments, 100  $\mu\text{L}$  of assay buffer (120 mM KCl, 1 mM  $\text{H}_2\text{KPO}_4$ , 10 mM MOPS, 20  $\mu\text{M}$  EGTA, 5 mM glutamate, 2.5 mM malate, pH 7.4) containing mitochondrial solution at 1 mg/mL was placed in each well of a 96-well plate. Then 100  $\mu\text{L}$  of assay buffer containing 300  $\mu\text{M}$   $\text{CaCl}_2$  was then added to the solution with a final concentration of 0.5 mg/mL for mitochondria and 150  $\mu\text{M}$   $\text{CaCl}_2$ . Mitochondrial swelling was then followed by measuring the change in absorbance at 540 nm using a spectrophotometer (Spectramax Plus-384, Molecular Devices, Sunnyvale, CA, USA), with a reading every 9 s/well for a total time of 10 min. Then 2  $\mu\text{L}$  of the compounds at the desired concentrations were added before the addition of the mitochondrial solution.

**Mitochondrial Calcium Retention Capacity (CRC) Assay.**<sup>29</sup> Mitochondrial CRC was assessed fluorimetrically in the presence of the fluorescent  $\text{Ca}^{2+}$  indicator Calcium Green SN (Molecular Probes C3737; ex-em 505–535 nm) using a temperature-controlled PerkinElmer LS 55 spectrofluorimeter. Mitochondria (0.5 mg) were diluted in 1 mL of CRC buffer (120 mM KCl, 1 mM  $\text{H}_2\text{KPO}_4$ , 10 mM MOPS, 20  $\mu\text{M}$  EGTA, 5 mM glutamate, 2.5 mM malate, pH 7.4) containing 1  $\mu\text{M}$  Calcium Green.  $\text{CaCl}_2$  (1  $\mu\text{L}$  of 2 mM stock) was added every minute to 200  $\mu\text{L}$  of the mitochondrial suspension, and its uptake was followed by measuring extra-mitochondrial calcium green fluorescence (PerkinElmer spectrofluorimeter at 25 °C) until mPTP opening was achieved. Compounds were added to the mitochondria immediately prior to the start of the experiment. CsA was used as positive control at a final concentration of 1  $\mu\text{M}$ .

**In Vivo Studies.** All aspects of animal care, use, and welfare for all animals used for in vivo studies were performed in strict compliance with the U.S. Department of Agriculture's (USDA) Animal Welfare (Rabbit experiment) or with EU and Italian Guidelines for Laboratory Animal Welfare (mouse and rat experiments).

**Ex Vivo CRC.** Mice hearts were excised, flushed with perfusion buffer (118 mM NaCl, 25 mM  $\text{NaHCO}_3$ , 4.7 mM KCl, 2.15  $\text{KH}_2\text{PO}_4$ , 0.6 mM  $\text{MgSO}_4$ , 1.69 mM  $\text{CaCl}_2$ , 11.1 mM glucose), and connected to a Langendorff reperfusion apparatus. Beating hearts were first perfused with perfusion buffer for 2 min prior to treatment and then with compound 22 at 5  $\mu\text{M}$  concentration with 0.1% DMSO in the perfusion buffer or DMSO (0.1% in perfusion buffer) for 2 min. Hearts were then immediately placed in ice followed by mitochondria preparation, and CRC evaluation was performed as described above.

**In Vivo Ischemia Reperfusion Injury in Rabbits.** New Zealand white rabbits were subjected to left anterior descending coronary artery ligation followed by reperfusion. Briefly, animals were anesthetized (30 mg/kg sodium pentobarbital iv), and a sternotomy was performed to visualize the left anterior descending artery (LAD). The LAD was temporarily ligated and maintained occluded for 30 min. At 5 min prior to reperfusion, the animals were administered compound 22 (5 mg/kg in 20% DMSO; 40% PEG400) or vehicle via iv bolus. At the end of the 30 min occlusion, the knot was loosened leaving the ligature in place, and the vessel was allowed to reperfuse for 4 h. At the end of the reperfusion period, each animal was injected intravenously (iv) with 8–10 mL of 0.5% Fast Green. The animals were euthanized, and the hearts were flushed with heparinized saline until cleared of blood. The hearts were cut into four slices which were photographed (cranial surface and caudal surface), along with a calibrated measurement block. The slices were then incubated in a 1% solution of triphenyltetrazolium chloride (TTC) in sodium phosphate buffer (pH 7.4) for 20 min at 37 °C. The heart rings were weighed and

photographed again. The sections of the heart were evaluated for area at risk (area of the heart perfused by the occluded artery) and infarct size using the photographs taken during necropsy. The images including the ruler were analyzed with ImageJ 1.32j software from the National Institutes of Health (NIH) and evaluated by group pairwise analysis (ANOVA).

**hERG Binding Assay.** Interaction with the hERG channel was assessed by displacement of the radioligand [ $^3\text{H}$ ]-astemizole as described by Chiu et al.<sup>36</sup>

**Assessment of Cardiovascular Parameters in the Conscious Rat.** Cardiovascular parameters were measured in conscious female rat following a single intravenous administration of compound 22 by means of a telemetry system (Data Science International, St. Paul, MN, USA). Animals used in this study had been instrumented about 1 week before the start of the study. Telemetry transmitters (model TL11M2-C50-PXT) implanted in the abdominal cavity allowed recording of blood pressure (via femoral artery) and body temperature.

Prior to the start of the study, animals were checked for general health status and for the functionality of the radio transmitters (readable and normal blood pressure waveform).

Cardiovascular parameters were collected from at least 1 h before treatment to about 24 h after treatment. The following parameters were calculated from the recorded blood pressure and body temperature waveforms: heart rate (bpm), systolic blood pressure (mmHg), diastolic blood pressure (mmHg), average blood pressure (mmHg), and body temperature (°C).

**Plasma Exposure in the Rabbit.** Blood samples were collected from the jugular vein of New Zealand white rabbits ( $n = 5$ ). Samples were collected predose and at 5, 15, 30, 60, and 240 min post reperfusion and placed in tubes containing  $\text{K}_2\text{EDTA}$  as anticoagulant. The blood samples were stored on an ice block until centrifuged. The plasma was collected and temporarily stored on dry ice until stored frozen at  $-50$  to  $-90$  °C until the analysis. Briefly, 100  $\mu\text{L}$  of plasma were added to a Sirocco filter plate (Waters) containing a mixture of ACN (300  $\mu\text{L}$ ) and 25%  $\text{H}_3\text{PO}_4$  (10  $\mu\text{L}$ ). The plate was shaken for 20 min and filtered under vacuum (15 mmHg) for 3 min. Sample analysis was performed on an Acquity UPLC injecting 5  $\mu\text{L}$  of the resulting solution on a Acquity HSS T3 column (50 mm  $\times$  2.1 mm  $\times$  1.8  $\mu\text{m}$ ,  $T = 40$  °C; eluent, water, ACN, 0.1% HCOOH gradient from 2% B to 100% B in 1.3 min flow 0.45 mL/min), coupled with a sample organizer and interfaced to a triple quadrupole Premiere XE (Waters, Milford, MA). The mass spectrometer was operated using electrospray interface (ESI) with a capillary voltage of 3.5 kV, cone voltage of 23 V, collision energy of 17 V, extractor 5 V, source temperature of 120 °C, desolvation gas flow of 800 L/h, and desolvation temperature of 480 °C. Collision energy was optimized for each compound. LC-MS/MS analyses were carried out using a positive electrospray ionization (ESI(+)) interface in MRM (multiple reaction monitoring) mode.

Plasma concentrations of compound 22 were extrapolated on an eight-point calibration curve (2.5–1000 ng/mL). QC samples of the test compound at three different concentrations (high, medium, and low) were considered for acceptance of the analytical runs with an accuracy within  $\pm 15\%$  except at the LLOQ of 2.5 ng/mL (lowest limit of quantification) where  $\pm 20\%$  was accepted.

Pharmacokinetic parameters were calculated by a noncompartmental method using WinNonLin 5.1 software (Pharsight, Mountain View, CA).

**Plasma Exposure in the Rat.** Blood samples were collected from the retro-orbital plexus of WI(Glx/BRL/Han)IGS rats. Samples were collected at 0.083, 0.332, 1, 2, 4, 7, and 24 h and placed in tubes containing  $\text{K}_2\text{EDTA}$  as anticoagulant. The blood samples were stored on an ice block until centrifuged. The plasma was collected and temporarily stored on dry ice until stored frozen at  $-50$  to  $-90$  °C until the analysis. The same sample preparation and analytical method developed for the rabbit (see above) was used to quantify compound 22 in the rat plasma.

## ■ ASSOCIATED CONTENT

### Supporting Information

CRC of mouse liver mitochondria after incubation with 0.1, 0.5, and 5  $\mu\text{M}$  inhibitor; synthesis and characterization of compounds 5–9, 13, 15–17, 19–23, 25–27, 30, 31, 33, 34, 10a, 14a, 18a, 25a, 26a, 27a–30a, 33a, and 34a; purity of key compounds as determined by HPLC;  $^1\text{H}$  NMR and UPLC traces of compounds 6 and 22; summary results of in vitro selectivity assays (compound 6); reactivity assay of compound 22 with *N*-acetyl cysteine or glutathione; plasma levels of 22 in the rat telemetry study. This material is available free of charge via the Internet at <http://pubs.acs.org>.

## ■ AUTHOR INFORMATION

### Corresponding Author

\*Phone: +39 02 9437 5128. Fax: +39 02 9437 5990. E-mail: [daniele.fancelli@ieo.eu](mailto:daniele.fancelli@ieo.eu).

### Present Addresses

$\circ$  Drug Discovery Program, Experimental Oncology Department, European Institute of Oncology IEO, Via Adamello 16, 20139 Milan, Italy.

$\blacklozenge$  Sbarro Health Research Organization—Center for Biotechnology, Temple University, 1900 North 12th Street, Philadelphia, Pennsylvania 19122–6099, United States.

$\text{¶}$  Fondazione Istituto Insubrico Ricerca per la Vita, Via R. Lepetit 34, 21040 Gerenzano, VA, Italy.

$\text{+}$  Teva Pharmaceuticals Fine Chemicals, Strada Statale Briantea, 23892 Bulciago, LC, Italy.

$\blacktriangle$  Translational Center for Regenerative Medicine, Fresenius Medical Care Italia SpA, Via Crema 8, Palazzo Pignano, CR, Italy.

$\square$  Aphad srl, Via della Resistanza 65, 20090 Buccinasco, MI, Italy.

$\diamond$  Flamma SpA, Via Bedeschi 22, 24040 Chignolo d'Isola, BG, Italy.

$\triangle$  Sigma-Tau Industrie Farmaceutiche Riunite SpA, Via Pontina, 00040 Pomezia, RM, Italy.

$\blacksquare$  Fondazione IRCCS, Istituto Neurologico Carlo Besta at IFOM Fondazione Istituto FIRC di Oncologia Molecolare, Via Adamello 16, 20139 Milan, Italy.

$\bullet$  Boehringer Ingelheim Pharma GmbH & Co. KG, Birkendorfer Strasse 65, 88397 Biberach an der Riss, Germany.

### Notes

The authors declare the following competing financial interests: SM and PGP are cofounder and stock holder of Genextra, a holding company that owns 100% of Congenia shares. SM and PGP are cofounder of Congenia. SM has been chief scientific officer of Congenia from 2004 to 2009; PB and MVa are stock holders of Genextra; most of the authors are former employees of Genextra, as indicated in the affiliations.

## ■ ACKNOWLEDGMENTS

We acknowledge the contribution of Mark Johnson at MPI Research (Mattawan, MI, US) for the in vivo rabbit study, Carlo Arrigoni at Accelerata (Nerviano MI, Italy) for the rat telemetry study, and Michel Ovize at Lyon University (Lyon, France) for helpful discussion and advice.

## ■ ABBREVIATIONS USED

AAR, area at risk; ACN, acetonitrile; CRC, calcium retention capacity; CsA, cyclosporine A; EDC, *N*-(3-(dimethylamino)propyl)-*N'*-ethylcarbodiimide hydrochloride; EGTA, ethylene

glycol-bis(2-aminoethyl ether)-*N,N,N',N'*-tetraacetic acid; EtOAc, ethyl acetate; FCCP, trifluorocarbonyl cyanide phenylhydrazide; HOBt, 1-hydroxybenzotriazole; IS, infarct size; LAD, left anterior descending; LRI, lethal reperfusion injury; MOPS, 3-(*N*-morpholino)propanesulfonic acid; mPT, mitochondrial permeability transition; mPTP, mitochondrial permeability transition pore; PCI, percutaneous coronary intervention; TTC, triphenyltetrazolium chloride

## ■ REFERENCES

- (1) Siemen, D.; Ziemer, M. What Is the Nature of the Mitochondrial Permeability Transition Pore and What Is It Not? *IUBMB Life* **2013**, *65*, 255–262.
- (2) Bernardi, P. The Mitochondrial Permeability Transition Pore: A Mystery Solved? *Front. Physiol.* **2013**, *4*, 95.
- (3) Halestrap, A. P. What Is the Mitochondrial Permeability Transition Pore? *J. Mol. Cell. Cardiol.* **2009**, *46*, 821–831.
- (4) Giorgio, V.; von Stockum, S.; Antoniel, M.; Fabbro, A.; Fogolari, F.; Forte, M.; Glick, G. D.; Petronilli, V.; Zoratti, M.; Szabó, L.; Lippe, G.; Bernardi, P. Dimers of Mitochondrial ATP Synthase Form the Permeability Transition Pore. *Proc. Natl. Acad. Sci. U. S. A.* **2013**, *110*, 5887–5892.
- (5) Azzolin, L.; von Stockum, S.; Basso, E.; Petronilli, V.; Forte, M. A.; Bernardi, P. The Mitochondrial Permeability Transition from Yeast to Mammals. *FEBS Lett.* **2010**, *584*, 2504–2509.
- (6) Hausenloy, D. J.; Boston-Griffiths, E. A.; Yellon, D. M. Cyclosporin A and Cardioprotection: From Investigative Tool to Therapeutic Agent. *Br. J. Pharmacol.* **2012**, *165*, 1235–1245.
- (7) Baines, C. P.; Kaiser, R. A.; Purcell, N. H.; Blair, N. S.; Osinska, H.; Hambleton, M. A.; Brunskill, E. W.; Sayen, M. R.; Gottlieb, R. A.; Dorn, G. W.; Robbins, J.; Molkenstin, J. D. Loss of Cyclophilin D Reveals a Critical Role for Mitochondrial Permeability Transition in Cell Death. *Nature* **2005**, *434*, 658–662.
- (8) Martin, L. J. The Mitochondrial Permeability Transition Pore: A Molecular Target for Amyotrophic Lateral Sclerosis Therapy. *Biochim. Biophys. Acta* **2010**, *1802*, 186–197.
- (9) Muirhead, K. E.; Borger, E.; Aitken, L.; Conway, S. J.; Gunn-Moore, F. J. The Consequences of Mitochondrial Amyloid Beta-Peptide in Alzheimer's Disease. *Biochem. J.* **2010**, *426*, 255–270.
- (10) Du, H.; Guo, L.; Zhang, W.; Rydzewska, M.; Yan, S.; Cyclophilin, D. Deficiency Improves Mitochondrial Function and Learning/Memory in Aging Alzheimer Disease Mouse Model. *Neurobiol. Aging* **2011**, *32*, 398–406.
- (11) Mazzeo, A. T.; Beat, A.; Singh, A.; Bullock, M. R. The Role of Mitochondrial Transition Pore, and Its Modulation, in Traumatic Brain Injury and Delayed Neurodegeneration after TBI. *Exp. Neurol.* **2009**, *218*, 363–370.
- (12) Yellon, D. M.; Hausenloy, D. J. Myocardial Reperfusion Injury. *N. Engl. J. Med.* **2007**, *357*, 1121–1135.
- (13) Dirksen, M. T.; Laarman, G. J.; Simoons, M. L.; Duncker, D. J. Reperfusion Injury in Humans: A Review of Clinical Trials on Reperfusion Injury Inhibitory Strategies. *Cardiovasc. Res.* **2007**, *74*, 343–355.
- (14) Jhund, P. S.; McMurray, J. J. Heart Failure after Acute Myocardial Infarction: A Lost Battle in the War on Heart Failure? *Circulation* **2008**, *118*, 2019–2021.
- (15) Morel, O.; Perret, T.; Delarche, N.; Labèque, J. N.; Jouve, B.; Elbaz, M.; Piot, C.; Ovize, M. Pharmacological Approaches to Reperfusion Therapy. *Cardiovasc. Res.* **2012**, *94*, 246–252.
- (16) Sharma, V.; Bell, R. M.; Yellon, D. M. Targeting Reperfusion Injury in Acute Myocardial Infarction: A Review of Reperfusion Injury Pharmacotherapy. *Expert Opin. Pharmacother.* **2012**, *13*, 1153–1175.
- (17) Piot, C.; Croisille, P.; Staat, P.; Thibault, H.; Rioufol, G.; Newton, N.; Elbelghiti, R.; Cung, T. T.; Bonnefoy, E.; Angoulvant, D.; Macia, C.; Raczk, F.; Sportouch, C.; Gahide, G.; Finet, G.; André-Fouët, X.; Revel, D.; Kirkorian, G.; Monassier, J.-P.; Derumeaux, G.; Ovize, M. Effect of Cyclosporine on Reperfusion Injury in Acute Myocardial Infarction. *N. Engl. J. Med.* **2008**, *359*, 473–481.

- (18) Rezzani, R. Cyclosporine A and Adverse Effects on Organs: Histochemical Studies. *Prog. Histochem. Cytochem.* **2004**, *39*, 85–128.
- (19) Freeman, D. J. Pharmacology and Pharmacokinetics of Cyclosporine. *Clin. Biochem.* **1991**, *24*, 9–14.
- (20) Mankad, P.; Spatenka, J.; Slavik, Z.; O'Neil, G.; Chester, A.; Yacoub, M. Acute Effects of Cyclosporin and Cremophor EL on Endothelial Function and Vascular Smooth Muscle in the Isolated Rat Heart. *Cardiovasc. Drugs Ther.* **1992**, *6*, 77–83.
- (21) N'guessan, B. B.; Sanchez, H.; Zoll, J.; Ribera, F.; Dufour, S.; Lampert, E.; Kindo, M.; Geny, B.; Ventura-Clapier, R.; Mettauer, B. Oxidative Capacities of Cardiac and Skeletal Muscles of Heart Transplant Recipients: Mitochondrial Effects of Cyclosporin-A and Its Vehicle Cremophor-EL. *Fundam. Clin. Pharmacol.* **2012**, *1*–10.
- (22) Waldmeier, P. C. Inhibition of the Mitochondrial Permeability Transition by the Nonimmunosuppressive Cyclosporin Derivative NIM811. *Mol. Pharmacol.* **2002**, *62*, 22–29.
- (23) Gomez, L.; Thibault, H.; Gharib, A.; Dumont, J.-M.; Vuagniaux, G.; Scalfaro, P.; Derumeaux, G.; Ovize, M. Inhibition of Mitochondrial Permeability Transition Improves Functional Recovery and Reduces Mortality Following Acute Myocardial Infarction in Mice. *Am. J. Physiol.: Heart Circ. Physiol.* **2007**, *293*, H1654–H1661.
- (24) Tiepolo, T.; Angelin, A.; Palma, E.; Sabatelli, P.; Merlini, L.; Nicolosi, L.; Finetti, F.; Braghetta, P.; Vuagniaux, G.; Dumont, J.-M.; Baldari, C. T.; Bonaldo, P.; Bernardi, P. The Cyclophilin Inhibitor Debio 025 Normalizes Mitochondrial Function, Muscle Apoptosis and Ultrastructural Defects in Col6a1<sup>-/-</sup> Myopathic Mice. *Br. J. Pharmacol.* **2009**, *157*, 1045–1052.
- (25) Reutenauer, J.; Dorchies, O. M.; Patthey-Vuadens, O.; Vuagniaux, G.; Ruegg, U. T. Investigation of Debio 025, a Cyclophilin Inhibitor, in the Dystrophic Mdx Mouse, a Model for Duchenne Muscular Dystrophy. *Br. J. Pharmacol.* **2008**, *155*, 574–584.
- (26) Schaller, S.; Paradis, S.; Ngoh, G. TRO40303, a New Cardioprotective Compound, Inhibits Mitochondrial Permeability Transition. *J. Pharmacol. Exp. Ther.* **2010**, *33*, 696–706.
- (27) Ricchelli, F.; Sileikytė, J.; Bernardi, P. Shedding Light on the Mitochondrial Permeability Transition. *Biochim. Biophys. Acta* **2011**, *1807*, 482–490.
- (28) Le Lamer, S.; Paradis, S.; Rahmouni, H.; Chaimbault, C.; Michaud, M.; Culcasi, M.; Afxantidis, J.; Latreille, M.; Berna, P.; Berdeux, A.; Pietri, S.; Morin, D.; Donazzolo, Y.; Abitbol, J.-L.; Pruss, R. M.; Schaller, S. Translation of TRO40303 from Myocardial Infarction Models to Demonstration of Safety and Tolerance in a Randomized Phase I Trial. *J. Transl. Med.* **2014**, *12*, 38.
- (29) Chem, J. B.; Fontaine, E.; Bernardi, P. A Ubiquinone-Binding Site Regulates the Mitochondrial Permeability Transition Pore. *J. Biol. Chem.* **1998**, *273*, 25734–25740.
- (30) Doherty, E. M.; Fotsch, C.; Bo, Y.; Chakrabarti, P. P.; Chen, N.; Gava, N.; Han, N.; Kelly, M. G.; Kincaid, J.; Klionsky, L.; Liu, Q.; Ognyanov, V. I.; Tamir, R.; Wang, X.; Zhu, J.; Norman, M. H.; Treanor, J. J. S. Discovery of Potent, Orally Available Vanilloid Receptor-1 Antagonists. Structure–Activity Relationship of *N*-Aryl Cinnamides. *J. Med. Chem.* **2005**, *48*, 71–90.
- (31) Germain, A. R.; Carmody, L. C.; Nag, P. P.; Morgan, B.; Verplank, L.; Fernandez, C.; Donckele, E.; Feng, Y.; Perez, J. R.; Dandapani, S.; Palmer, M.; Lander, E. S.; Gupta, P. B.; Schreiber, S. L.; Munoz, B. Cinnamides as Selective Small-Molecule Inhibitors of a Cellular Model of Breast Cancer Stem Cells. *Bioorg. Med. Chem. Lett.* **2013**, *23*, 1834–1838.
- (32) Tamiz, a P.; Cai, S. X.; Zhou, Z. L.; Yuen, P. W.; Schelkun, R. M.; Whittemore, E. R.; Weber, E.; Woodward, R. M.; Keana, J. F. Structure–Activity Relationship of *N*-(Phenylalkyl)cinnamides as Novel NR2B Subtype-Selective NMDA Receptor Antagonists. *J. Med. Chem.* **1999**, *42*, 3412–3420.
- (33) Xiao, Y.; Yang, X.; Li, B.; Yuan, H.; Wan, S.; Xu, Y.; Qin, Z. Design, Synthesis and Antifungal/Insecticidal Evaluation of Novel Cinnamide Derivatives. *Molecules* **2011**, *16*, 8945–8957.
- (34) Yoya, G. K.; Bedos-Belval, F.; Constant, P.; Duran, H.; Daffé, M.; Baltas, M. Synthesis and Evaluation of a Novel Series of Pseudo-Cinnamic Derivatives as Antituberculosis Agents. *Bioorg. Med. Chem. Lett.* **2009**, *19*, 341–343.
- (35) Basso, E.; Fante, L.; Fowlkes, J.; Petronilli, V.; Forte, M. A.; Bernardi, P. Properties of the Permeability Transition Pore in Mitochondria Devoid of Cyclophilin D. *J. Biol. Chem.* **2005**, *280*, 18558–18561.
- (36) Chiu, P. J. S.; Marcoe, K. F.; Bounds, S. E.; Lin, C.-H.; Feng, J.-J.; Lin, A.; Cheng, F.-C.; Crumb, W. J.; Mitchell, R. Validation of a [<sup>3</sup>H]Astemizole Binding Assay in HEK293 Cells Expressing HERG K<sup>+</sup> Channels. *J. Pharmacol. Sci.* **2004**, *95*, 311–319.